A THEORETICAL MODEL FOR LIPID BILAYER PHASE TRANSITIONS AND PHASE DIAGRAMS

By

WOOD HI CHENG

Bachelor of Science
Tamkang College of Arts and Sciences
Tamsui, Taiwan
1968

Master of Science
National Tsinghua University
Hsinchu, Taiwan
1970

Submitted to the Faculty of the Graduate College
of the Oklahoma State University
in partial fulfillment of the requirements
for the Degree of
DOCTOR OF PHILOSOPHY
May, 1978

A THEORETICAL MODEL FOR LIPID BILAYER PHASE

TRANSITIONS AND PHASE DIAGRAMS

Thesis Approved:

Hugh L. Scott
Thesis Adviser

Paul Westhaus

J P Chandler

Richard C. Essenberg

Norman N. Durham
Dean of the Graduate College

ACKNOWLEDGMENTS

The author wishes to express his appreciation and gratitude to his major adviser, Dr. H. L. Scott, for the suggestion of this problem and for his patient guidance and encouragement throughout the entire study.

Thanks are also extended to the members of my committee, Dr. J. P. Chandler, Dr. R. C. Essenberg, and Dr. P. A. Westhaus, for their help and advice, and particularly to Dr. Chandler for the use of his subroutine STEPIT.

The author gratefully acknowledges the financial support provided by the National Science Foundation and the Department of Physics at Oklahoma State University.

Finally, I wish to express special thanks to my wife, Shu-Chu, and our daughter, Shaio-Wei, for their understanding, inspiration and love.

TABLE OF CONTENTS

LIST OF TABLES

LIST OF FIGURES

Figure Page

LIST OF SYMBOLS

Symbol	
A	Total Area Per Molecule
A_i	Assigned Area
A_o	Ground-State Area
C	Attractive Energy Constant
DMPC	Dimyristoylphosphatidylcholine
DPPC	Dipalmitoylphosphatidylcholine
DSPC	Distearoylphosphatidylcholine
DBPC	Dibehenoylphosphatidylcholine
E_{att}	Attractive Energy
E_{h-c}	Hard-Core Energy
E_{rot}	Rotational Energy
F	Helmholtz Free Energy
G	Gibbs Free Energy
g_i	Average Number of Gauche Rotations
H	Model Hamiltonian
ΔH	Enthalpy Change
K	Boltzmann Constant
N	Total Number of Molecules
S	Packing Entropy
SPT	Scaled Particle Theory
T	Temperature

W_i	Weights
X	Mole Fraction of Molecules
α_i	Fraction of Molecules
μ_i	Chemical Potential
π	Surface Pressure

CHAPTER I

INTRODUCTION

Historical Background

The fundamental unit of most living organisms is the cell. Every living cell is enclosed by membranes which play a crucial role in many cellular phenomena. The typical cell membrane is made up of phospholipids with their hydrophilic heads forming outer layers in contact with water and their hydrophobic tails meeting at the center of the membranes. The basic structure of a phospholipid molecule is shown in Figure 1. In addition to lipids, proteins are also major components of membranes. Because the phospholipids found in biological membranes are the basic structure of cell membranes, the physical properties of phospholipids have been the subject of a large volume of recent work. One of the important physical properties of this work is the demonstration by X-ray diffraction (1), differential scanning calorimetry (2-4), dilatometry (5), light scattering (6,10), NMR (7-8), ESR (9-10), infrared spectra (11), Raman spectra (12), and fluorescent labeling (6,13) techniques, that phospholipid bilayers undergo thermotropic transitions from a crystalline state at low temperature to a liquid crystalline state at high temperature. The Arrhenius plots for transport (14-16) or enzyme (17-19) activities found in biological membranes of unsaturated fatty acid auxtrophs of E. coli also exhibit discontinuities at or near the associated lipid phase transition. Such a change in state may play an

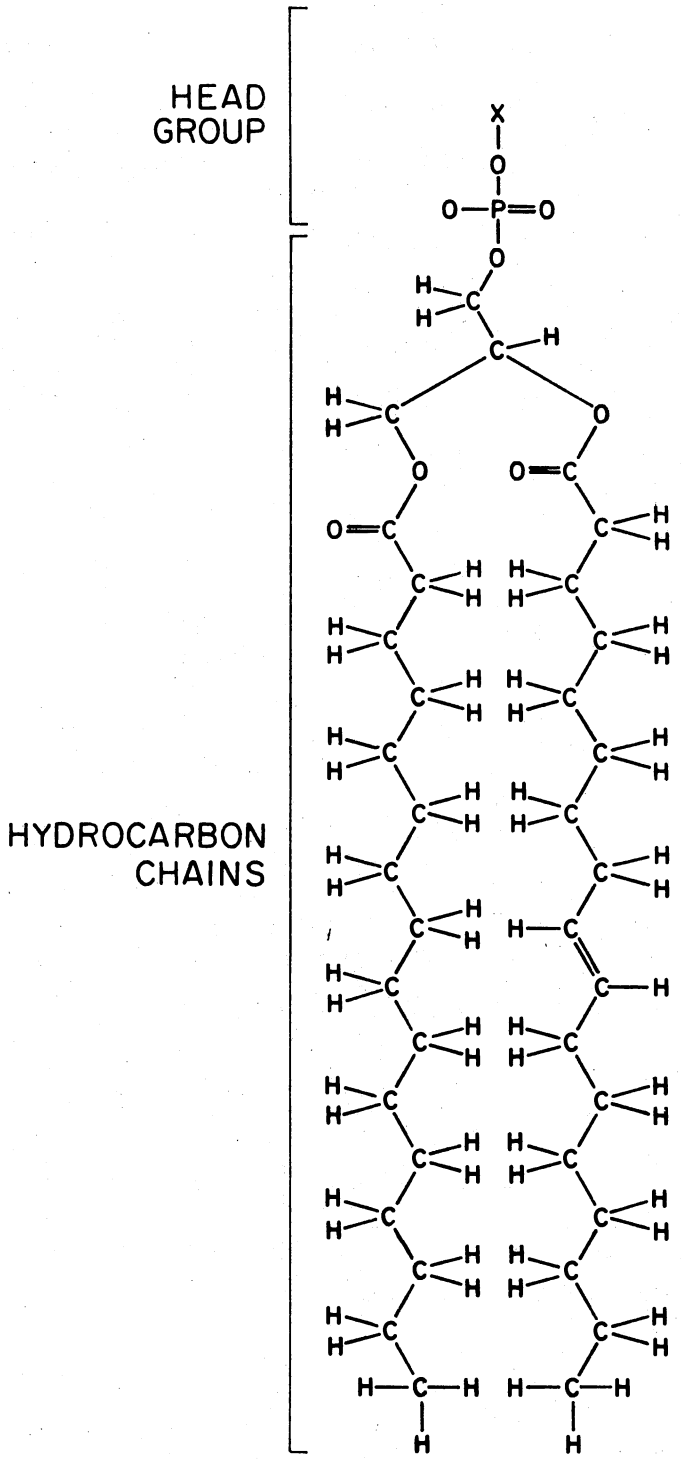

Figure 1. The Typical Structure of a Phospholipid Molecule. A Phospholipid is Composed of a Hydrophilic Head Group and Two Hydrocarbon Tails. The X Component in the Head Group Usually is Different for Different Phospholipids, and the Number of Carbons in Chain May Vary Also

important structural and functional role in such cell membrane properties as transport and enzyme activities, lipid-protein interactions, and physiological process.

Here, we review briefly some results from basic techniques such as X-ray diffraction, calorimetry, ESR and dilatometry published in the literature concerning the membrane phase transitions. Differential scanning calorimetry measurements show that the specific heat of distearoyl L-α lecithin has a sharp peak with a width of about 2°C centered around 55°C and a latent heat of about 10.8 Kcal/mol (2). This technique also shows that a second broader transition is observed at lower temperature than the main transition. The main transition specifies the melting of the hydrocarbon chains of lipid bilayers, a strongly cooperative process in which the hydrocarbon chains go from an ordered state to a disordered state. The lower transition, as suggested by Ladbrooke and Chapman (20), reflects a rotation of the polar head portion of the lipid molecules. X-ray diffraction (1,17) studies show that below the transition temperature the lipid hydrocarbon chains are almost perpendicular to the plane of bilayer and close-packed in a quasi-hexagonal two-dimensional lattice with an interchain separation of about 4.2 Å. However, above the transition temperature the lipids are in a fluid state that gives a diffraction pattern which indicates a separation of about 4.6 Å. The replacement of a sharp band at 4.2 Å with broad band at 4.6 Å above the transition temperature indicates that the hydrocarbon chains change their conformation from a closely packed hexagonal array to a liquid-like state. ESR (9) studies also show increased disorder of the hydrocarbon chains in the high temperature phase. Recently, density measurements using dilatometry indicate that two phase transi-

tions take place in lecithins, a sharp main transition and a lower transition (5). The main phase transition has been interpreted as similar to the melting transition in alkanes from the crystalline phase to the liquid phase.

The interpretation of the experimental results on the chain melting transition (also called the chain order-disorder transition) is that the main phase transition in pure lipid bilayers and in biological membranes involves cooperative gauche rotations among the hydrocarbon chains of the lipids (21). A gauche rotation is formed by rotating a straight hydrocarbon chain about a particular carbon-carbon bond by a angle of $\pm$ 120^{o}. From the rotational isomerism (22), it is known that each C-C bond in a hydrocarbon chain has three possible conformations. There is one trans conformation t (ψ = 0^{o}) and two gauche conformations g^{+} and g^{-} (ψ = $\pm$ 120^{0}). Figure 2 illustrates the structures of trans and gauche conformations of lipid bilayers.

Recently, phase changes in binary mixtures of lipids and the biological membranes have been discussed in terms of phase separations (3,15,22-28). According to the studies of Shimshick and McConnell (23), phase diagrams representing lateral phase separation in the plane of a lipid bilayer can be described as two-dimensional equilibria between the fluid and solid phases. The binary mixtures of lipids do not undergo a single, sharp phase transition, but a much broader transition in which the equilibrium between the fluid and solid phases can coexist over a finite range of temperatures. It has been shown by Shimshick and McConnell (23) that the lateral phase separation in a lipid bilayer should have a high compressibility could facilitate the insertion of proteins, ions, or new membranes into the old membrane without large

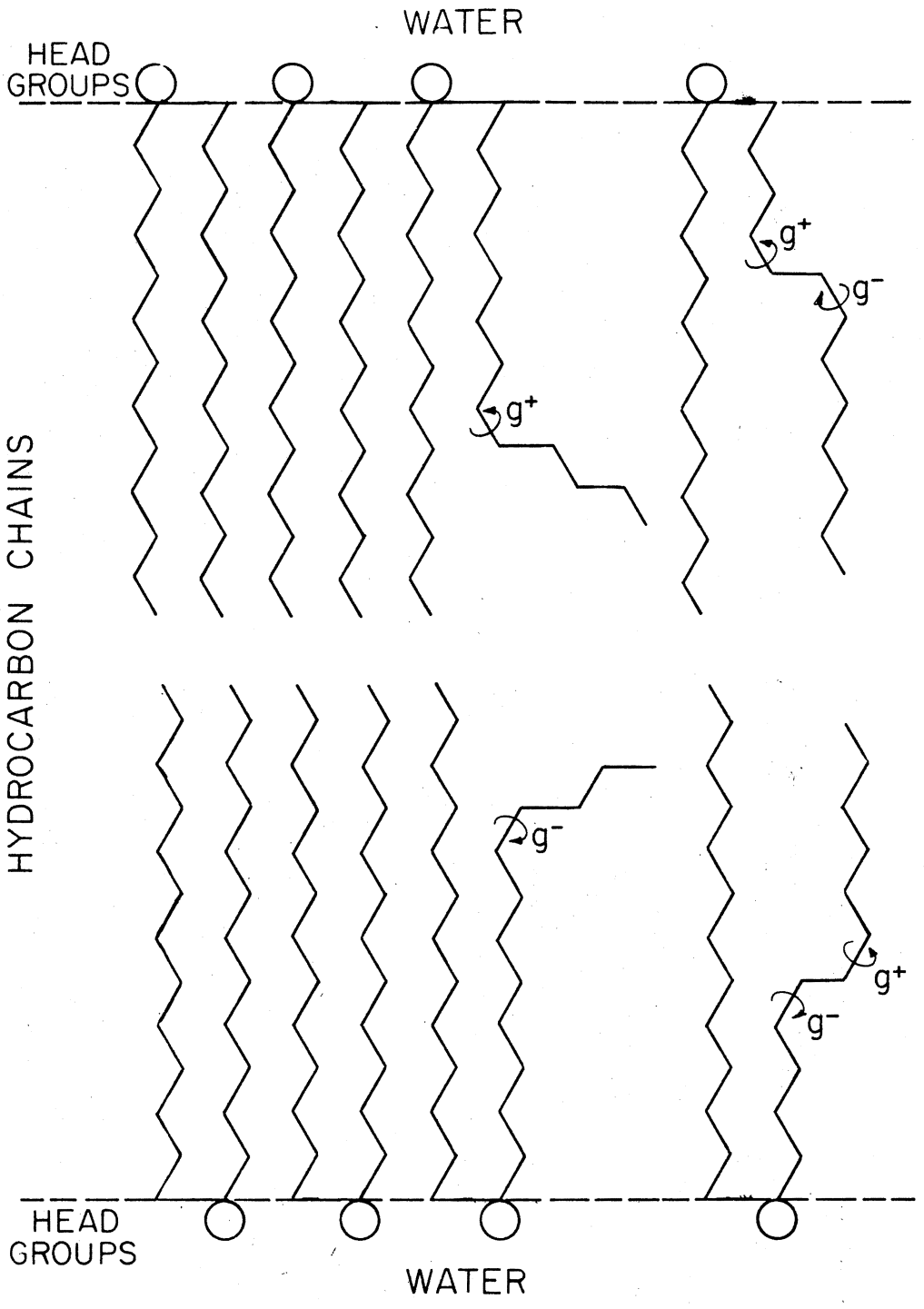

Figure 2. A Schematic Diagram of the Trans and Gauche Conformations of Lipids in a Bilayer. The Zig-Zag Lines Represent the Hydrocarbon Chains and the Circles Represent Head Groups. The Two Lipids on the Left are in All-Trans Conformations. The Chains in the Middle Have One Gauche Rotation. The Chains on the Right Have Two Gauche Rotations

expansions in membrane area and enhance the activity of transport systems.

Numerous studies have shown that cholesterol molecules incorporated into the phospholipid bilayer have a profound influence on hydrocarbon chains (12,29-32). Early calorimetric (29) studies of cholesterol-dipalmitoylphosphatidylcholine mixtures showed a decrease in the transition enthalpy, eventually vanishing at 50 mole percent cholesterol. Recent studies on dipalmitoylphosphatidylcholine and dimyristoylphosphatidylcholine dispersions indicate that the transition enthalpy decreases linearly with the percentage of cholesterol and vanishes at about 33 mole percent cholesterol (30). A variety of proteins have been studied for their ability to interact and affect the phase transitions of lipid bilayers (33-37). Papahadjopoulos et al. (33) have classified some membrane proteins on the basis of their effects on lipid phase transitions. Group 1, including ribonuclease and polylysine, tends to increase the transition enthalpy without changing the transition temperature. Group 2 proteins, including cytochrone c, strongly decrease both the heat of transition and the transition temperature. Group 3 proteins, including gramicidin A, decrease the transition without strongly affecting the transition temperature. Recently, calorimetric studies of the gramicidin A-dipalmitoylphosphatidylcholine mixtures showed a decrease in the transition enthalpy vanishing at about 12 mole percent gramicidin A (37).

Summary of Current Research

A theoretical treatment of phase transitions in lipid bilayers and biomembranes is complicated, because there are many different degrees

of freedom involved of both intramolecular and intermolecular nature. The hard core constraints and the long range attractive forces lead to great mathematical difficulties which have only been solved approximately. At the present time, there have been many theoretical models (38-49) dealing with lipid bilayer and biomembrane phase transitions. The first quantitative theoretical description of lipid bilayer phase transitions was due to Nagle (38). Nagle has considered two basic models, one called model A which can be transformed to a dimer model and the other called model B which like model A can also be transformed to dimer model but has a different geometry of dimer states. These models then allow exact solutions using dimer techniques. Using the dimer techniques which treat the case of infinite hydrocarbon chains confined to two-dimensional lattices, Nagle calculated exactly the packing entropy for a line of very long chains. Together with the rotational isomerism and attractive long range forces, the Nagle model exhibits phase transitions which can be comapred to the chain order-disorder transitions in DPL. The results of Nagle's model do not contain any parameters or assumptions about the cooperative behavior of system. Nagle (39-40) has recently extended his model to the description of monolayer transitions and the effect of headgroup interactions on the lipid monolayer and bilayer phase transitions. In his studies of the behavior between monolayer and bilayer phase transitions, Nagle (40) makes an argument that monolayers under a surface pressure of 50 dynes/cm should be the same as bilayers. This behavior will play a useful role in our model when we determine the attractive energy constants and surface pressure of lipid bilayers.

Marčelja (41) has presented a theory for chain ordering in lipid

bilayer stability. According to the Marčelja model, the energies (forces) of a hydrocarbon chain in a bilayer are the internal energy of a single chain in a given conformation, the dispersive energy between neighboring hydrocarbon chain, and the lateral pressure on each chain. In his model the energies of each of the possible conformational states of a single chain are treated in a molecular field approximation of neighboring chains. Then he calculates the chain ordering in a self-consistent method by exact summation over all allowed single-chain states. Marčelja's treatment of the intermolecular interaction is similar to the Maier-Saupe method for liquid crystals. The results of the pressure-area diagrams, the order parameter for hydrocarbon chain as a function of temperature, lateral pressure and position along the chain are calculated and compared with the experimental data. The technique used by Marčelja has been successfully applied to the even-odd effect in liquid crystals with CH_2 end chains (50).

Scott (42-43) has proposed a theory, which is similar to that used by Alben to analyze a lattice model for biaxial liquid crystals, for the treatment of the hard-core forces in monolayer phase transition. In his treatments of hard-core forces, Scott first designates a set of possible molecular shapes to accommodate the kinks or jogs of hydrocarbon chains, and then constructs the number of lattice cells to be packed with the CH_2 groups. He also assigns a statistical weight to each class corresponding to the number of isomeric states consistent with molecular shape associated with that class. Upon addition of a long range attractive energy and a rotational isomeric energy to the total energy, Scott's model exhibits monolayer phase transitions. The results of theoretical pressure-area isotherms are similar to the experimental data of Phillips

and Chapman (51). Scott has successfully modified his model to account for the difference between transition temperature in phosphatidylcholines and phosphatidylethanolamines (44). In his studies of monolayer phase transitions (43-44), Scott has presented an hypothesis that the hydrocarbon chain region and the head group-water interface are effectively energetically isolated. Recently, the results of Monte Carlo computer experiments have supported this hypothesis (52).

Anderson et al. (45) have presented a theoretical model which makes use of mean field and scaled particle theory. Like the above models this model includes the excluded volume interactions, the chain conformation energy, and the long range interactions. The long range interactions have been expressed as a mean field energy. The excluded volume interaction between head groups has been assumed to be equivalent to the Hamiltonian for hard disks in two dimensions. They then use the high density expansion for hard disks to find the partition function of interactions among head groups. The excluded volume interaction between chains has also been expressed as product of the effect lateral pressure and cross-sectional area. This treatment is similar to the model of Nagle (38) and Marčelja (41) except that Anderson et al. use an approach motivated by the scaled particle theory to describe the interaction between chains. Using two adjustable parameters, Anderson et al.'s model gives enthalpy and area changes that agree with experimental data (2, 22). The approach of Anderson et al. is, like that of Scott (42-43), an attempt to consider the hard core steric forces as carefully as possible for systems which more closely resemble actual monolayers or bilayers than those for which Nagle (38) performs exact calculations. Recently, Anderson et al. have generalized their one-component model to

two-component bilayers (46). In their two-component model the partition function has been written as a function of area, composition, temperature, the average coordinate of head groups, the average height of chains, and the mean square height of chains. After minimization of the Gibbs energy at fixed temperature and composition and using a double tangent construction method, Anderson et al.'s model yields phase diagrams which are in good agreement with the experimental data (3,23).

Let us summarize briefly the other theoretical models for lipid bilayer phase transitions. McCammon and Deutch (47) have developed a model in which they deal with kinks and more liquid-like disorder contributions from the region near the ends of chains. Their treatment of intermolecular interaction is based on the Bragg-Williams approximation. The model has been applied to predict the melting temperature of single-component bilayers and the phase diagrams of two-component bilayers. Marsh (48) has studied the rotational states of a single lipid molecule and the steric interactions between two chains. Using the matrix method described by Flory (21), the Marsh model gives kink concentrations that are in agreement with the molecular permeability theory of Trauble (53). Jackson (49) has presented a theoretical model which uses the assumption that the β-coupled gauche kinks are the only nonstraight hydrocarbon chain conformations allowed. The results of Jackson's model can reproduce the experimental data of chain melting transition by using two adjustable parameters.

Purpose of This Study

The major goal of this work is to present a reliable model with semiempirical potentials to replace the intermolecular interactions for

single component lipid bilayer phase transition, observed in the homologous series of 1, 2-diacylphosphatidylcholines. These phospholipids are dimyristoylphosphatidylcholine(DMPC), dipalmitoylphosphatidylcholine (DPPC), distearoylphosphatidylcholine(DSPC), and dibehenoylphosphatidylcholine(DBPC). Then the model may be extended to the description of lipid mixtures, lipid-cholesterol, and lipid-protein systems which can provide a closer understanding of biological membranes than the single component systems. The paper we present here is related to the model studied by Anderson et al. (45), Nagle (38), and Scott (42-43). The chain conformation energy in our calculations is similar to Scott's model (42-43), but differs from Scott's model slightly in that chain conformation energies are calculated by considering kinks and jogs which seem to be among the most common rotational isomeric states in closely packed monolayers and bilayers. The long range attractive force is the same as the Nagle (38) and Scott (42-43) models in that they use van der Waals attractive energy to describe the long range interactions. But our model differs from the Nagle and Scott models in that the attractive energy is modified by replacing the area of the lipid bilayer by an effective area which accounts for the excluded volume part of the model. The excluded volume interaction between molecules we use in our calculations is related to Anderson's model (45), but the SPT is directly applied to find packing entropy of hard-core interaction between molecules without making any additional approximations about the interchain steric repulsions. It seems that improved theoretical models must carefully consider the hard-core interchain repulsive forces, and in this paper we make use of the fact that the SPT approach seems to be a very good approximation for treatment of hard-core interchain interactions.

In Chapter II we describe the method of calculation for pure systems. In Chapter III we generalize the model to the two-component systems. Chapter IV gives the results of our analysis and a discussion of the results. Chapter V contains our conclusions.

CHAPTER II

METHODS OF CALCULATION FOR ONE-COMPONENT SYSTEMS

A potentially useful method for finding an approximate Hamiltonian to describe a complex system such as a lipid bilayer is to replace the exact intermolecular interactions by semiempirical potentials which treat the individual interactions separately. In view of the results of experimental studies of phase transitions from an ordered structure to a disordered structure in membranes (1-19) and the theoretical consideration of the type of forces present in lipid bilayers and biomembranes (54), it seems reasonable to propose a theoretical model for which we can write an effective Hamiltonian for a monolayer or half a bilayer in the form

$$H = H_{att} + H_{rot} + H_{h-c} \tag{1}$$

These are basically the same energy contributions to monolayers as used Anderson et al. (45), Marčelja (41), Nagle (38) and Scott (42-43). The first term, H_{att}, is the sum of attractions holding monolayers together. The second term, H_{rot}, is the internal energy of the chain configuration. According to the well-known rotational isomeric model (21), each carbon-carbon bond can take up either a trans conformation with energy $\varepsilon = 0$ or one of two gauche conformations with energy $\varepsilon = 500$ cal/mol. The last term, H_{h-c}, is the excluded volume interactions among the

molecules. The approximate Hamiltonian which simplifies the intermolecular interactions of lipid bilayers will be obtained by using the results of quantum chemical calculations of long range forces, the rotational isomeric theory, and the scaled particle theory of fluid mixtures in the next three parts.

Packing Entropy

The experimental properties of lipids in monolayers and bilayers provide several hints for the development of new models. For example, the rather large mobility of lipids within the plane of a monolayer (10,55-57) suggests that relatively little entanglement of chains between molecules occurs. This, together with an almost constant order parameter over most of the chains (58-59) suggests a model in which most gauche bonds occur pairwise (kinks or jogs) which move rapidly up and down a chain. This would imply that lipid molecules with rapidly moving kinks can be approximately treated as cylinders whose radius or area is proportional to the number of kinks. Another consequence of this treatment is that there is only a finite number of allowed radii for the cylinders. That is, the total number of lipid molecules in cylinders of different areas can be writeen as $\sum_i \alpha_i N$ where N is the total number of lipid molecules; α_i denotes the fraction of molecules in cylinder state i which is determined by the number of kinks, and $\sum_i \alpha_i = 1$. If the cylinders are infinitely hard, then the packing of different states of lipid molecules in a two dimensional layer is identical to the packing of a two dimensional system of hard disks of varying radius.

We use scaled particle theory (60), described in Appendix A, to find the pressure and chemical potential of our mixture of hard disks.

Combining the pressure and chemical potential we obtain the Helmholtz free energy, and the entropy is then given by

$$S/NK = 1 - \sum_{i=1} \alpha_i \ln(\alpha_i) + \ln(A/N - \sum_{i=1} \alpha_i A_i) - \frac{(\sum_{i=1} \alpha_i \sqrt{A_i})^2}{(A/N - \sum_{i=1} \alpha_i A_i)} \quad (2)$$

Here A_i is the area assigned to the state i, A is the total area and N is the total number of molecules in the system. The summation in this equation goes over all the different states of hard-core system.

Treatment of Rotational Isomerism

After finding the packing entropy the next procedure is to define the allowed conformation states for lipids in our model. As we described previously, deuterium label experiments show an almost constant order parameter over most of the chains (58-59). A region of constant order parameter requires the same angular fluctuation for all segments involved. This result implies that the occurrence of an isolated gauche conformation is relatively rare. More common are the pairwise kinks or jogs which leave the chains parallel to each other. The kink ($g^{\pm} tg^{\mp}$) is formed from a straight hydrocarbon chain by rotating about a particular C-C bond by a angle of 120° and rotating either of the two next nearest neighboring C-C bonds by -120° (53,61). In the formation of one kink two trans configurations in the CH_2 chain are transformed into gauche configurations and the chain is shortened by one CH_2 unit length (59). Kinks are mobile structural defects which can move up and down the hydrocarbon chain with diffusion coefficient $D_{eff} \approx 10^{-5}$ cm^2/sec (53). We also allow states of form jogs (g..ttt...g), discussed by Seelig and Pechhold (59,62). The jog states may also move up and down along the

chain. By formation of jog, the chain is shortened by ½(n+1) CH_2 units where n is the number of trans segments between the two gauche segments.

There are fourteen bonds per chain for DMPC. We consider only twelve of these units as rotatable (we exclude the top and last units), since experiments show the CH_2 chains are rigid and tightly packed near the polar group (63-64). Applying the kink and jog isomeric models we suggest six possible configurations for DMPC, as indicated schematically in Figure 3. To compensate for not explicitly including all possible states we assigned weights W_i to each state according to the number of chain conformations possible for a chain of area associated with state i. In Table I various chain state, weight per chain, total weight and average number of gauche rotations for the state of DMPC are listed which in accordance with kink or jog isomeric models (59,62). According to the kink model, a simple counting shows there are 10 ways to place one kink (2 g1), 30 ways to place two kinks (2 (2 g1)), and 20 ways to place three kinks (3 (2 g1)). For jogs, there are 8 ways to place 2g2jog, 6 ways to place 2g3jog, 4 ways to place 2g4jog, and 2 ways to place 2g5jog. We also allow jog states of the form 3g2, 3g3, 4g3, 4g4, 5g4, 3g5, 4g5, 5g5, and 6g5, of jog. The agb is an isomeric state of jog where a is the total number of gauche conformations and b is the shortening of the chain in the CH_2 units. If we use these values then, for example, state 3 which two kinks, 2g2jog, and 3g2 may be formed in 2 x 30 + 10 x 10 + 2 x 8 + 2 x 8 = 192 ways since one may have either both kinks on one chain or on one kink, 2g2jog and 3g2 on each chain. The average number of gauche rotations, g_i, in Table I are found by weighted sums over all states of the given radius. The above model allowed six possible configurations of DMPC analogous to the states

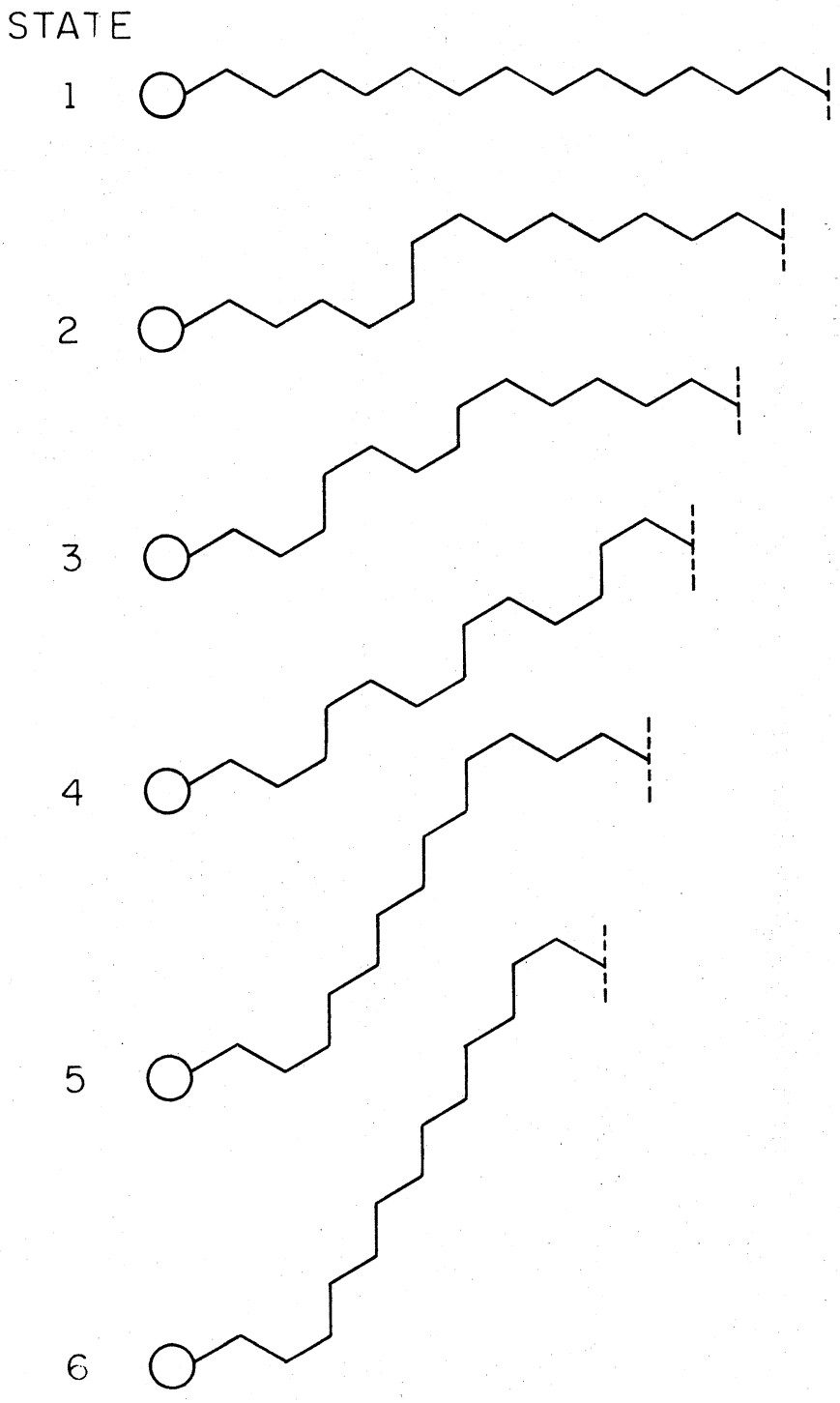

Figure 3. A Kink Model for a Lipid Bilayer (DMPC). Here We Show Lipids Only With One Chain. The Circles Indicate the Head Groups and the Zig-Zag Lines Indicate the CH_2 Chains

TABLE I

CHAIN STATE, STRUCTURAL DEFECT, WEIGHT PER CHAIN, TOTAL WEIGHT AND AVERAGE NUMBER OF GAUCHE ROTATIONS FOR THE STATE OF DMPC

State	Structural Defect	Weight Per Chain	Total Weight for the State	Average Number of Gauche Rotations for the State
	a b			
1	ogo Tran	1	1	0
2	2g1 Kink	10	20	2
3	2(2g1) Kinks	10 x 6/2! = 30	192	3.75
	2g2jog	8		
	3g2	8		
4	3(2g1) Kinks	10 x 6 x 2/3! = 20	676	5.84
	2g3jog	6		
	3g3	6		
	4g3	6		
5	2g4jog	4	192	4.75
	3g4	4		
	4g4	4		
	5g4	4		
	2(2g2jog)	8 x 2/2! = 8		
	2(3g2)	8 x 2/2! = 8		
6	2g5jog	2	20	4
	3g5	2		
	4g5	2		
	5g5	2		
	6g5	2		

a. The first number gives the total gauche conformations.

b. The second number indicates the shortening of chain in unit of i = 1.25 $\mathring{A}^2$ and the expansion of the equation $A_i = A_o \frac{L_o}{L_o - i}$.

shown in Figure 3. By the same reasoning, we consider a seven-state model for DPPC, an eight-state model for DSPC, and a nine-state model for DBPC. The various chain states, total number of weights and total number of gauche rotations in each state are given by Tables II, III and IV. This set of molecular shapes of DMPC, DPPC, DSPC, and DBPC we hope will conform to most of the possible shapes of lipids in monolayers. These shapes are designed to accommodate the kinks and jogs in chains which seem to be among the most common rotational isomeric states in closely packed monolayers and bilayers (55,59).

Now we must assign the area A_i to the model. Experiments show that the volume change accompanying bilayer phase transition was less than 5% (5,65-66). From this fact it seems reasonable to approximate the average areas as functions of chain length by

$$A_i L_i = A_o L_o \tag{3}$$

Here L_o is the length of hydrocarbon chain in all-trans configuration with an average cross-sectional area $A_o = 40.8$ Å (41,67-68). A_i and L_i are the effective cross-sectional area and length of a given configuration i respectively.

From the equation (3) the cross-section of a given chain configuration is given by

$$A_i = \frac{A_o L_o}{L_i} \tag{4}$$

This expression is identical to that used by Marčelja (41).

Since there are six possible states of DMPC and each allowed state corresponds to one assigned area, we have six assigned areas of DMPC.

TABLE II

CHAIN STATE, WEIGHT AND NUMBER OF GAUCHE ROTATIONS OF DPPC

State	Weight	Number of Gauche Rotations
1	1	0
2	24	2
3	280	3.79
4	1,328	5.90
5	328	4.78
6	256	4.84
7	24	4.50

TABLE III

CHAIN STATE, WEIGHT AND NUMBER OF GAUCHE ROTATIONS OF DSPC

State	Weight	Number of Gauche Rotations
1	1	0
2	28	2
3	384	3.81
4	5,240	5.97
5	9,456	7.83
6	1,116	5.42
7	728	4.58
8	28	5

TABLE IV

CHAIN STATE, WEIGHT AND NUMBER OF GAUCHE ROTATIONS OF DBPC

State	Weight	Number of Gauche Rotations
1	1	0
2	36	2
3	1,612	3.94
4	5,460	5.96
5	33,184	7.91
6	132,580	9.83
7	3,684	5.96
8	4,660	6.16
9	1,312	6.93
10	36	6

These six areas assigned to DMPC from the equation (4) are simply given by

$$A_i = 40.8 \frac{14}{14 - i} \tag{5}$$

where i = 0, 1, 2, 3, 4, 5.

Similarly, for DPPC:

$$A_i = 40.8 \frac{16}{16 - i} \tag{6}$$

where i = 0, 1, 2, 3, 4, 5, 6

DSPC:

$$A_i = 40.8 \frac{18}{18 - i} \tag{7}$$

where i = 0, 1, 2, 3, 4, 5, 6, 7

DBPC:

$$A_i = 40.8 \frac{22}{22 - i} \tag{8}$$

where i = 0, 1, 2, 3, 4, 5, 6, 7, 8, 9.

Attractive Energy

As we mentioned earlier, the effective Hamiltonian contains three terms. With the exception of H_{rot}, the other two terms in the Hamiltonian involve interactions between lipid molecules. We have replaced the exact intermolecular interaction by a semiempirical potential, so that each lipid molecule is imagined to be a hard disk surrounded by an attractive force field. Then the repulsive (H_{h-c}) and attractive (H_{att}) energies may be considered separately. The hard-core interactions among

the molecules have approximated by the SPT expression. Now we must treat the attractive part of lipid molecules.

The attractive dispersion forces can be calculated by perturbation theory (69-71). We consider the interaction of two neutral molecules for which the intermolecular distance is large compared with molecular dimensions. The first-order and second-order perturbation between permanent moments and induced moments vanishes, because nonpolar molecules cannot have permanent moments. The first nonvanishing second-order perturbation yields dispersion forces which correspond to induced dipole-induced dipole interactions. The van der Waals dispersion forces between macromolecules at small distance have been recognized as a contributing factor to the stability of many biological structures in which two or more long molecular chains are found to be only a few $\mathring{A}$ apart (54). It is clear that dispersion forces are important in maintaining the lipid-bilayer chains in the cell membranes.

The attractive energy between two long parallel hydrocarbon chains has been calculated by Salem (54) who used two assumptions: pairwise additivity of dispersion forces between groups on each chain, and isotropy of polarizability of a group on the chains. The result was given by

$$E = -\frac{C^1}{r^5} \tag{9}$$

where C^1 is the attractive energy constant. This is the attractive energy between long saturated chains at short distance r which we use in our lipid bilayer model.

The total attractive energy or van der Waals interaction energy in

a two-dimensional layer is given by, in a continum approximation,

$$E = -\frac{C^2}{r_o^3} = -\frac{C^3}{A^{3/2}} \tag{10}$$

where r_o is the average chain separation, and C^2 and C^3 are related to the van der Waals energy constant. The power 3 results from a $\frac{1}{r^5}$ attractive energy which is integrated over the two-dimensional layer. The average CH_2 group separation r_o is proportional to the cross-sectional area $A^{1/2}$.

The main effect of the hard core is to forbid the presence of any other molecule in a certain volume about a particular molecule. If A is the total area occupied by a lipid bilayer, the effective area available to one of its lipid molecules would be smaller than A by the totality of such excluded volumes, $A_{eff} = A - A_o$ where A_o is a constant depending on the molecular dimension. Therefore, in this paper we use an attractive energy of the form

$$E_{att} = -\frac{C}{(A - A_o)^{1.5}} \tag{11}$$

where A is the area per molecule, A_o is a constant, and C is an effective interaction constant, to be evaluated semiempirically.

Let us consider the ratio of the excluded volume energy to the attractive energy in our model and take the limit as the packing of lipid molecules approach as the ground state. From equations (2) and

(11), this limit r can be written approximately as

$$r = \lim_{A \to 40.8} \left| \frac{1/(A - 40.8)}{1/(A - A_o)^{1.5}} \right| \tag{12}$$

As part of our semiempirical construction, we expect that the excluded volume interaction effect should be stronger than the long range interaction in determining the bilayer phase transitions. That is, the r should be greater than 1 and hence, A_o should be smaller than 40.8. In this case it is reasonable to choose A_o = 38 $\mathring{A}^2$/molecule as a fixed parameter. This figure is slightly less than 40.8 $\mathring{A}^2$/molecule used for the ground state in equations (5-8), which allows for a slight softening of the hard cores. In order to consider the hard-core effect and have consistency in our model, the scaled particle expressions dictate that a singular potential of the form of equation (11) be used, or no phase transitions will occur.

Having found the average number of gauche rotations, g_i, and the assigned area, A_i, we now wish to calculate the rotational energies for each isomeric state of DMPC. First, we assign an energy ε = 500 cal/mole for each gauche rotation (22). Then using Table I, the rotational energies in our calculations are 0, $N\alpha_2(2\varepsilon)$, $N\alpha_3(3,75\varepsilon)$, $N\alpha_4(5.84\varepsilon)$, $N\alpha_5(4.75\varepsilon)$, and $N\alpha_6(4\varepsilon)$ for state 1, 2, 3, 4, 5 and 6 of DMPC. Recall the α_i denotes the fraction of lipid molecules in state i and N is the total number of lipid molecules. Similarly, we can calculate the rotational energies of DPPC, DSPC, and DBPC.

The Helmholtz Energy

The Helmholtz free energy of half of a lipid bilayer for DMPC, ac-

cording to the equation $F = F_{rot} + F_{att} - TS$ can be written

$$F/NK = \frac{500}{RT}\left(\sum_{i=1}^{6} g_i\alpha_i\right) - \frac{C(14)}{RT(A - 38)^{1.5}} - \left\{1 - \sum_{i=1}^{6} \alpha_i \ln(\alpha_i/W_i)\right.$$

$$\left. + \ln\left(A - \sum_{i=1}^{6} \alpha_i A_i\right) - \frac{\left(\sum_{i=1}^{6} \alpha_i \sqrt{A_i}\right)^2}{\left(A - \sum_{i=1}^{6} \alpha_i A_i\right)}\right\} \qquad (13)$$

All the summations in this equation are over all the various states of DMPC. The parameters g_1, W_i, and A_i are determined from our previous discussions in Table I. Similarly we can obtain the free energies of DPPC, DSPC, and DBPC. The summations in these free energies go over all various seven, eight, and ten states for DPPC, DSPC, and DBPC, respectively. These parameters g_i, W_i, and A_i are determined from Tables II, III, and IV.

The numerical analysis involves finding the values of the α_i which minimize the free energy at fixed temperature and area. The minimization was performed using the subroutine STEPIT written by J. P. Chandler, Computer Science Department, Oklahoma State University. The model we present here has two adjustable energy parameters, the difference between the trans and gauche rotation energy and the van der Waals attractive energy. The first parameter is set at 500 cal/mol, in the first term in equation (13), in accordance with experiment (21). In keepting with the semiempirical nature of our model, the second parameter C is adjusted so that our calculated isotherms agree as closely as possible with the experiment. For heat of sublimation at $0^{o}K$ of linear paraffin chains the van der Waals energy constant, 1.84 Kcal/mol CH_2 (39,54), can be used to test the results. In our model we first determine the isothermal

properties of system, and then we use these properties to consider the melting transition in bilayers.

For calculation of the surface pressure, we use the Helmholtz free energy, $F = E - TS$, and the thermodynamic law $TdS = dE + \pi dA$. Then the surface pressure π is obtained by the usual thermodynamic formula

$$\begin{aligned} \pi &= -\left(\frac{\partial F}{\partial A}\right)_T \\ &= -(NKT)\left(\frac{\partial (F/NKT)}{\partial A}\right)_T \end{aligned} \tag{14}$$

The numerical calculation of the surface pressure is performed using the following relation

$$\pi = -(NKT) \lim_{\Delta A \to O} \left\{\frac{(F/NKT)_{A+\Delta A} - (F/NKT)_{A-\Delta A}}{2\Delta A}\right\}$$

$$= -N \times 1.38 \times 10^{-16} \ (\text{erg}/^{o}\text{K}) \times T(^{o}\text{K}) \lim_{\Delta A \to O} \left\{\frac{(F/NKT)_{A+\Delta A} - (F/NKT)_{A-\Delta A}}{2\left(\frac{\Delta A}{N}\right) N(10 \times 10^{-16} \ \text{cm}^2)}\right\}$$

$$= -(1.38\ T) \lim_{\Delta A \to O} \left\{\frac{(F/NKT)_{A+\Delta A} - (F/NKT)_{A-\Delta A}}{2\Delta A}\right\} \tag{15}$$

For ease of comparison to the experimental results, the values π and A are given in the conventional units of dynes/cm and A^{o2}/molecule, respectively.

We can obtain a set of isotherms for any value of the interaction constant C. Making use of Nagle's argument that bilayers are similar to monolayers at about 50 dynes/cm (40) we adjust C so that, at the bilayer transition temperature, the monolayer transition at this pressure

has an enthalpy change which agrees with the experimental bilayer result.

The pressure-area isotherms for phosphatidylcholines are shown in Figures 4, and 5 for four the temperatures 279, 314, 328, and 348^{o}K. These monolayer isotherms are characterized by van der Waals loops which, after Maxwell construction, lead to coexisting phases in a first order transition. The values of van der Waals energy constants determined from these isotherms are 116, 132, 148, and 175 Kcal/mole for DMPC, DPPC, DSPC, and DBPC respectively.

To compare with the experimental data 1.84 Kcal/mole CH_2 for the heat of sublimation at 0^{o}K of long paraffin chains, to the value obtained by calculation we use equation (11). From equation (11) the attractive energy for ground state is given by

$$E_{\substack{\text{ground}\\\text{state}}} = - \frac{CN}{(40.8 - 38)^{1.5}} \qquad (16)$$

where C is the attractive energy constant and N is the number of CH_2 groups in each chain. Then the attractive energy constants determined from this equation are 0.88, 0.88, 0.88 and 0.85 Kcal/mole CH_2. Because the DMPC, DPPC, DSPC, and DBPC bilayers contain relatively short alkyl chains in bilayers the values of energy constants in our calculations are smaller than the experimental 1.84 Kcal/mole CH_2 for very long linear paraffin chains. In the pressure-area isotherms, the phase transition begins at area A_e in the expended phase and ends at area A_c in the condensed phase. The two differences between these two states, $A_c - A_e$ is the surface area change.

For the calculation of the enthalpy change at the transitions, we use

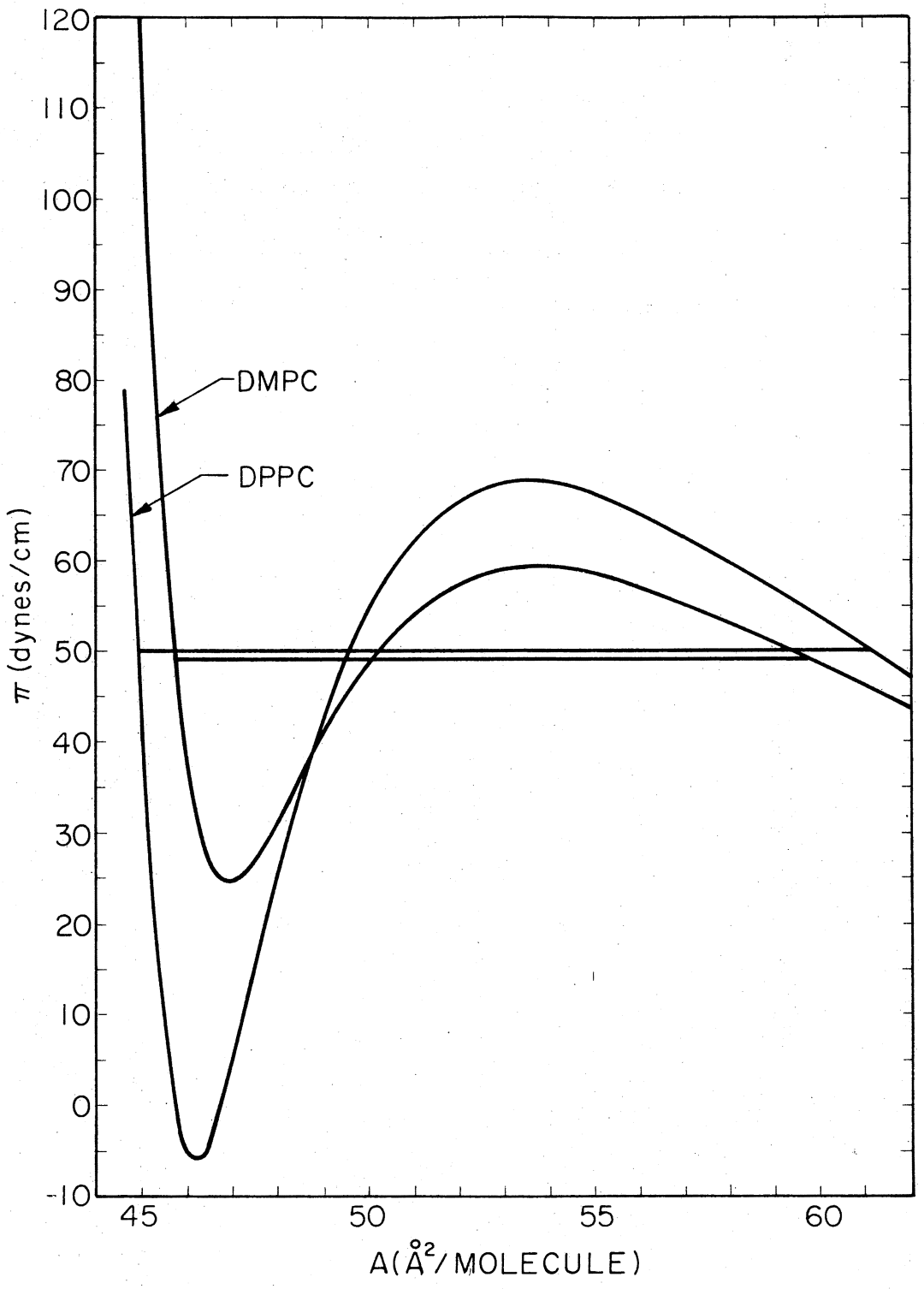

Figure 4. A Plot of Pressure-Area Isotherms, for DMPC and DPPC Lipids in Monolayers at Temperatures, 297 and 314°K Respectively. The Attractive Energy Constants in the Model are 0.88 and 0.88 Kcal/mole CH_2 for DMPC and DPPC Respectively

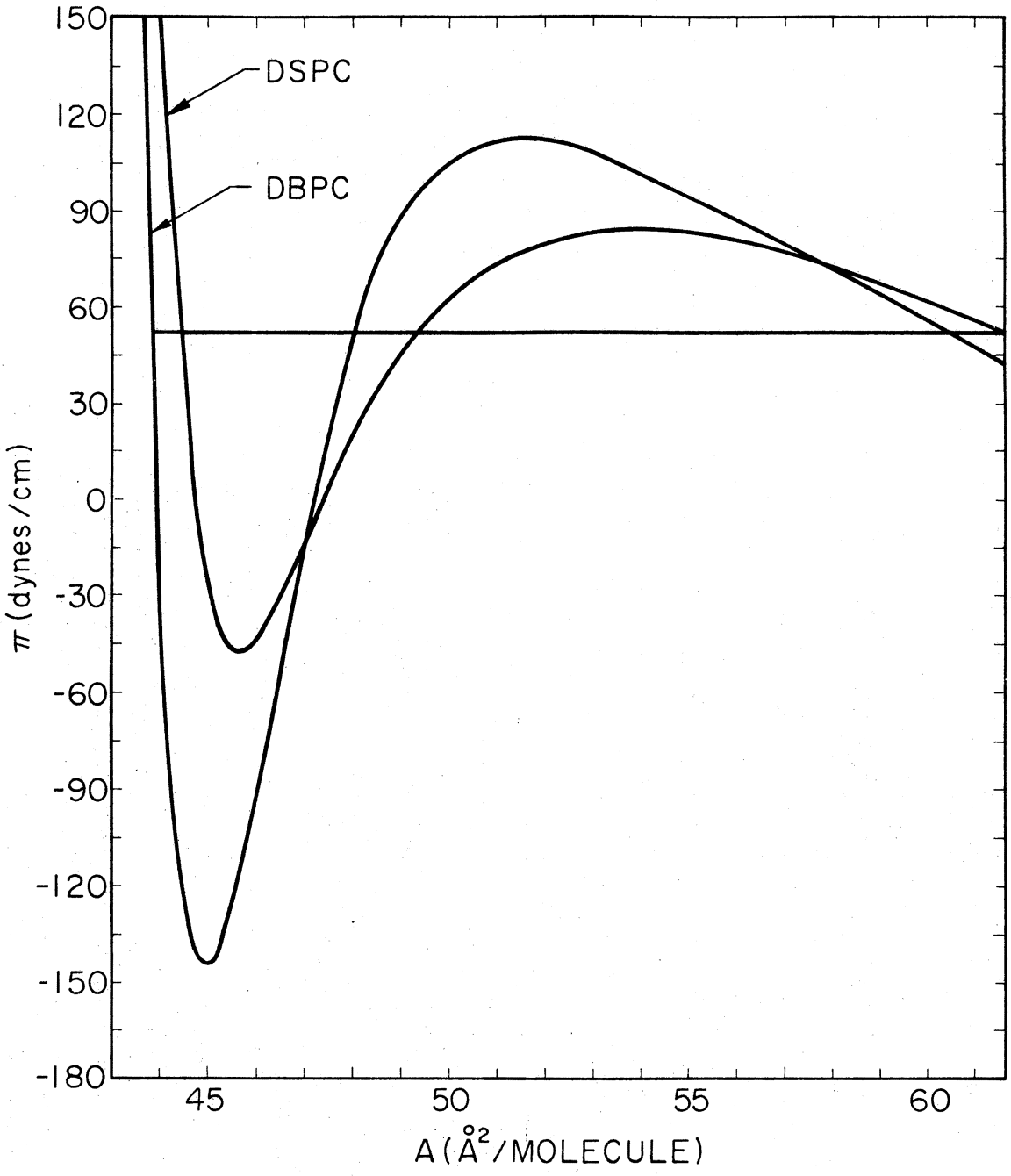

Figure 5. The Pressure-Area Isotherms for DSPC and DBPC Lipids in Monolayers at Temperatures, 328 and 348°K Respectively. The Attractive Energy Constants in the Model are 0.88 and 0.85 Kcal/mole CH_2 for DSPC and DBPC Respectively

$$\Delta H = T\Delta S \tag{17}$$

where ΔS is the entropy change. The change of entropy at the phase transition can be obtained by minimization of Gibbs free energy at fixed T and π. The Gibbs free energy has the form

$$G = E_{int} + E_{att} - (1.44 \text{ cal/mol})\pi A - TS \tag{18}$$

where 1.44 cal/mol is conversion factor to convert πA into cal/mol CH_2.

Then the equation of entropy change is given by

$$\begin{aligned}
\Delta S/NK &= \left(\frac{\partial G}{\partial T}\right)_{A_c} - \left(\frac{\partial G}{\partial T}\right)_{A_e} \\
&= \left(1 - \sum_i \alpha_i \ln(\alpha_i/W_i) + \ln\left(A - \sum_i \alpha_i A_i\right) - \frac{\left(\sum_i \alpha_i \sqrt{A_i}\right)^2}{\left(A - \sum_i \alpha_i A_l\right)}\right)_{A_c} \\
&\quad - \left(1 - \sum_i \alpha_i \ln(\alpha_i/W_i) + \ln\left(A - \sum_i \alpha_i A_i\right) - \frac{\left(\sum_i \alpha_i \sqrt{A_i}\right)^2}{\left(A - \sum_i \alpha_i A_i\right)}\right)_{A_e}
\end{aligned} \tag{19}$$

We will discuss the enthalpy changes, the area changes, and the surface pressures in Chapter IV.

CHAPTER III

METHODS OF CALCULATION FOR TWO-COMPONENT SYSTEMS

Binary Mixtures of Lipid

The theoretical model of a single lipid component phase transitions is only the first step towards an understanding of structural changes in biological membranes. Molecular heterogeneity in naturally occurring membranes causes their transitions to broaden and become lower in enthalpy (3,22-28). Such broadened transitions observed experimentally can be studied in model systems such as lipid mixtures. There are currently two theoretical models (46,47) concerned with phase diagrams in binary mixtures of lipid.

Let us consider binary systems with the components denoted by A and B. The system A contains N_A molecules and B contains N_B molecules. The relative concentration of A is $X_A = N_A/(N_A + N_B)$; B is $X_B = N_B/(N_A + N_B)$. We are concerned with the case in which the two components have a common head group but differ in the number of CH_2 groups. As before we consider the lipid molecules to be a mixture of hard disks such that the total number of lipid molecules $N_A + N_B = N$ is fixed and the total number of states is the sum $N_S = N_{A,S} + N_{B,S}$. Here $N_{A,S}$ and $N_{B,S}$ are the number states of component A and B respectively. Then the packing entropy of two components is given by

$$S/NK = 1 - \sum_{i=1}^{N_S} \alpha_i \ln(\alpha_i/W_i) + \ln(A - \sum_{i=1}^{N_S} \alpha_i A_i) - \frac{(\sum_{i=1}^{N_S} \alpha_i \sqrt{A_i})^2}{(A - \sum_{i=1}^{N_S} \alpha_i A_i)} + X_A \ln X_A + X_B \ln X_B \tag{20}$$

where

$$X_A = \sum_{i=1}^{k} \alpha_i$$

$$X_B = 1 - X_A$$

$$= \sum_{i=k+1}^{N_S} \alpha_i$$

Now if we assume that the total attractive energy can be written as a sum of pair energies, we shall have

$\frac{X_A^2}{2} E_{AA}$ pair energy of type AA

$\frac{X_B^2}{2} E_{BB}$ pair energy of type BB

$X_A X_B E_{AB}$ pair energy of type AB

Then the total attractive energy will be

$$E_{att} = - \frac{C(A)\ X_A^2 + C(B)\ X_B^2 + [C(A) + C(B)]\ X_A\ X_B}{(A - 38)^{1.5}} \tag{21}$$

where the factors of ½ are contained in the constants C(A) and C(B),

since a similar pairwise summation was done in obtaining the single particle attractive energy, equation (11). C(A) and C(B) are van der Waals energy constants for the respective one-component systems. In this case, the pair energy of type AB, E_{AB}, equals to C(A) + C(B).

According to our assumptions, the total free energy of two-component bilayers for DMPC - DPPC mixtures is given by

$$F/NKT = \frac{500}{RT}\left(\sum_{i=1}^{13} g_i\alpha_i\right) - \frac{C(14)\,X_{14}^2 + C(16)\,X_{16}^2 + (C(14) + C(16))\,X_{14}\,X_{16}}{RT(A - 38)^{1.5}}$$

$$- \left\{1 - \sum_{i=1}^{13} \alpha_i \ln(\alpha_i/W_i) + \ln\left(A - \sum_{i=1}^{13} \alpha_i A_i\right) - \frac{\left(\sum_{i=1}^{13} \alpha_i \sqrt{A_i}\right)^2}{\left(A - \sum_{i=1}^{13} \alpha_i A_i\right)}\right.$$

$$\left. - X_{14} \ln X_{14} - X_{16} \ln X_{16}\right\} \qquad (22)$$

The summations in this equation from one to seven correspond to DPPC states and from eight to thirteen correspond to DMPC states. Here X_{16}, the fixed DPPC composition, equals the sum of $\{\alpha_i\}$ corresponding to states of DPPC molecules, and X_{14}, equals the sum of $\{\alpha_i\}$ corresponding to states of DMPC molecules, such that $X_{16} + X_{14} = 1$ is fixed. As before, the parameters g_i, W_i, and A_i are determined from our previous discussions. Similarly, we can obtain the free energies of DMPC - DPPC, and DPPC - DSPC mixtures. The summations in these free energies go over all fourteen and fifteen states for DMPC - DSPC and DPPC - DSPC respectively.

Area-Composition Diagrams for Mixed Lecithin Monolayers

As we presented in the previous section, the one-component monolayers graphs of pressure-area isotherms for a given temperature as a function of composition (short length) are constructed. Then the plots of molecular area versus composition shown in Figures 6, 7, and 8 represent the mixture of lecithin monolayers. Figures 6, 7, and 8 show mean molecular area-composition diagrams for mixed DPPC - DSPC, DMPC - DSPC, and DMPC - DPPC respectively at temperature 295 ^{o}K and at pressure 5 dyne/cm; 20 dyne/cm.

Phase Diagrams

A common way to describe the binary phase equilibria between the solid and fluid phases is to use the T - X curves (72). The condition of equilibrium between these two phases is given by

$$\begin{aligned} T^{solid} &= T^{fluid} \\ \pi^{solid} &= \pi^{fluid} \\ \mu_i^{solid} &= \mu_i^{fluid} \end{aligned} \tag{23}$$

where T is the temperature, π is the surface pressure, and μ_i is the chemical potential.

The model defined by equation (22), cannot satisfy this condition and produce a binary phase diagram, because plots of the Gibbs free energy versus composition are always convex. Therefore, we phenomeno-

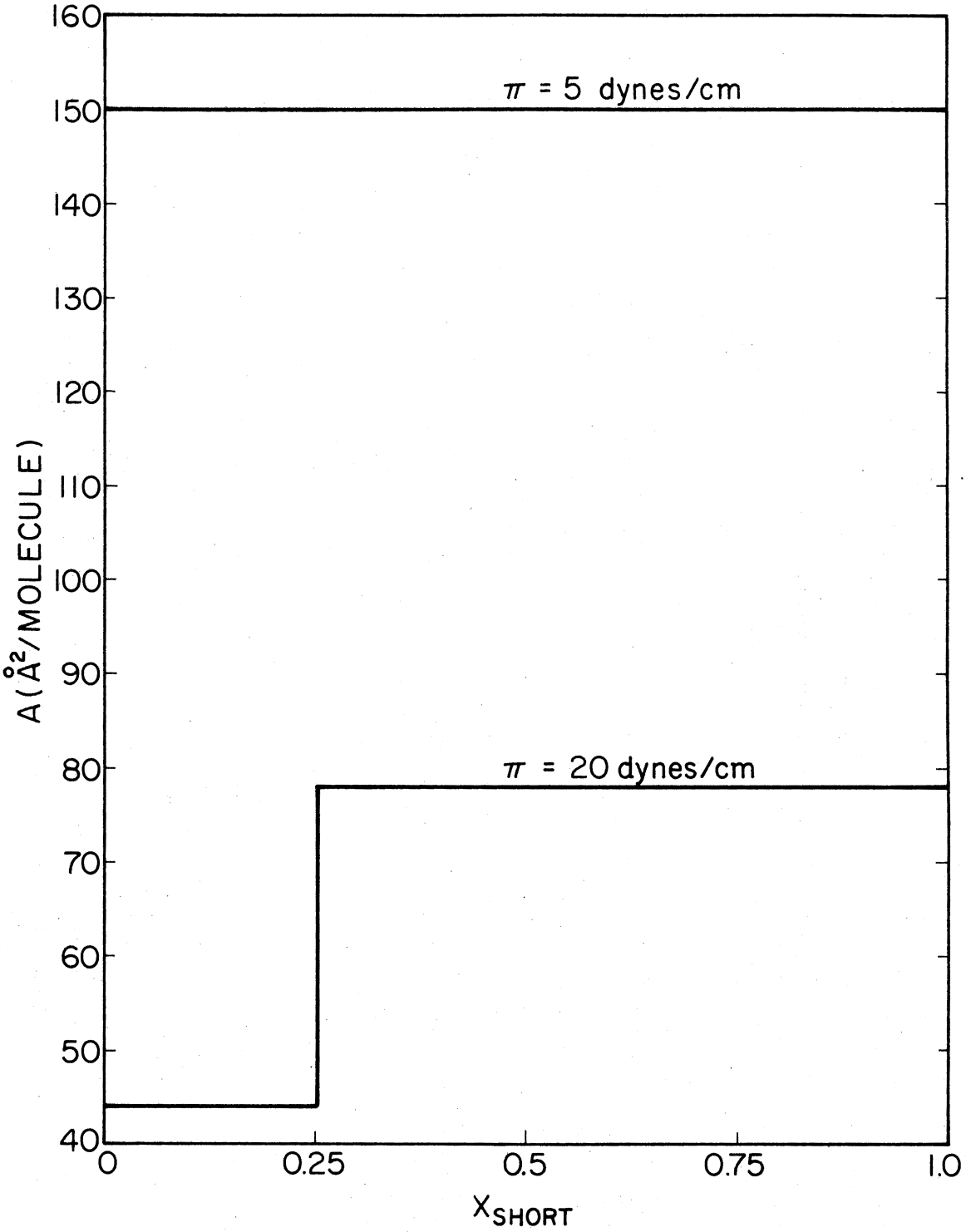

Figure 6. A Plot of Area Per Molecule vs. Mole Fraction of Short Chain Component for a Mixed Monolayer of DPPC-DSPC Phospholipids at T = 295°K. The Step in 20 Dynes/cm Data Lower Curve is Due to the First Order Transition at X_{short} = 0.25. The Upper Curve Corresponds to a Surface Pressure of 5 Dynes/cm

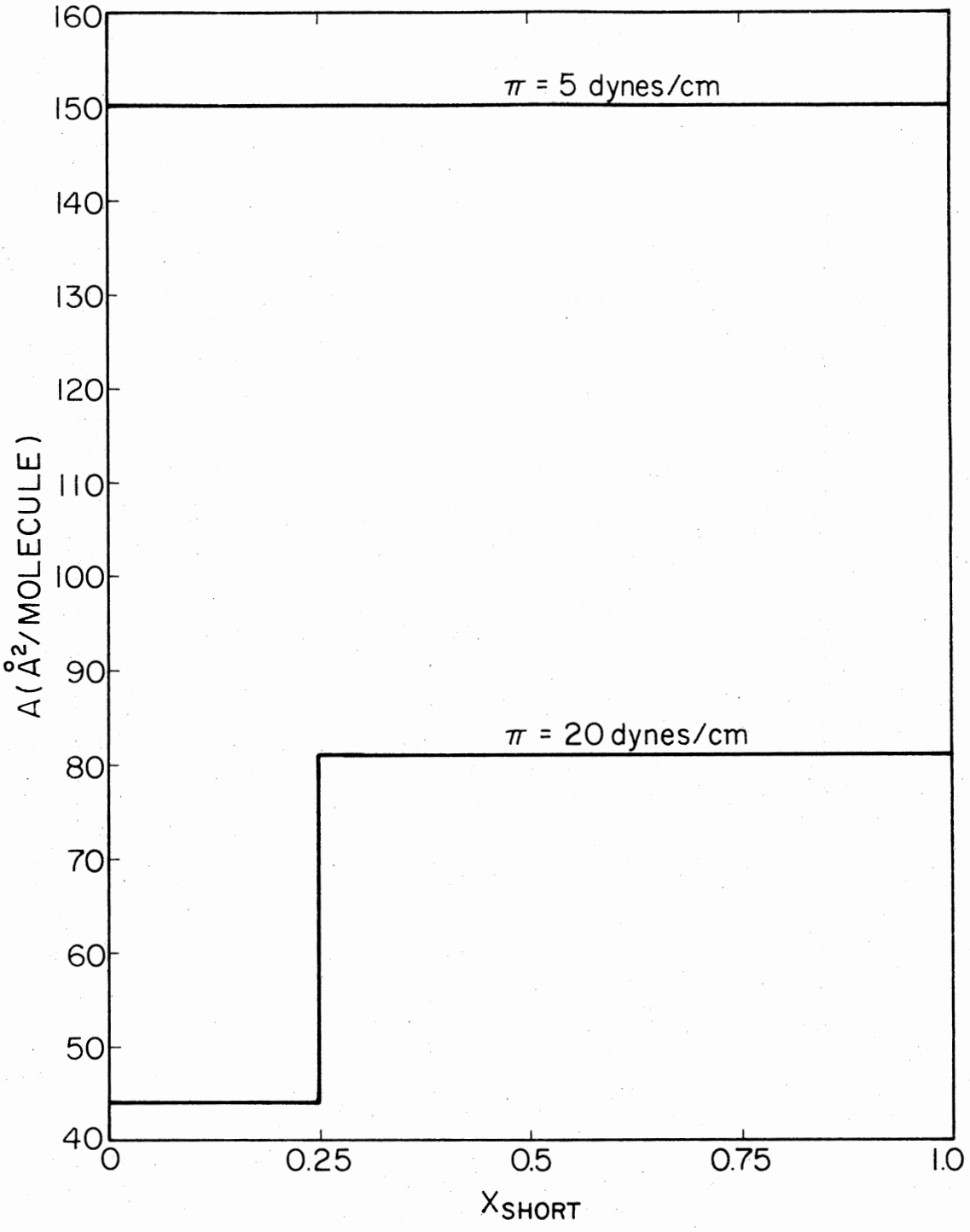

Figure 7. A Plot of Area Per Molecule vs. Mole Fraction of Short Chain Component for a Mixed Monolayer of DMPC-DSPC Lipids, at T = 295°K. The Step in 20 Dynes/cm Data Lower Curve is Due to the First Order Transition at $X_{short} = 0.25$. The Upper Curve Corresponds to a Surface Pressure of 5 Dynes/cm

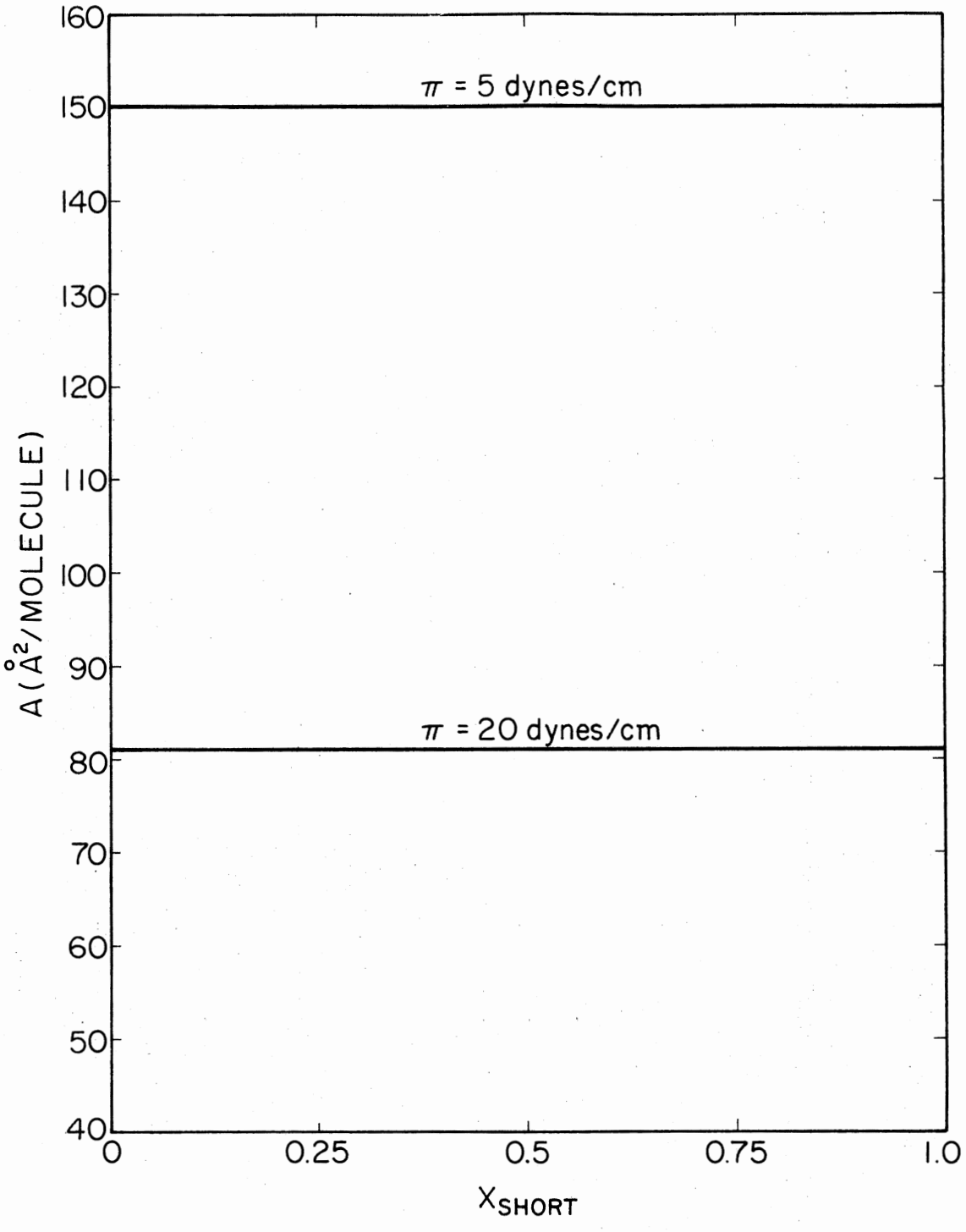

Figure 8. A Plot of Area Per Molecule vs. Mole Fraction of the Short Chain Component for a Mixed Monolayer of DMPC-DPPC Lipids, at T = 295°K. The Upper Curve Represents a Surface Pressure 5 Dynes/cm and the Lower Curve Represents a Surface of 20 Dynes/cm

logically obtain phase diagrams in the following manner. At fixed T, N, and A, we minimize the free energy for each X. Graphs of pressure-area isotherms as a function of X^{solid} (long chain) and X^{fluid} (long chain) for given T are found. The temperatures we use in our calculations correspond to experimental values (3,22). The surface pressure at coexistence for a given temperature is found by using Maxwell construction. The chemical potential for a given temperature can be calculated by Gibbs free energy, $\mu = G = F + \pi A$. Then the composition X^{solid} and X^{fluid} at equilibrium must be such that T, π, and μ_i have the same values for solid and fluid phases.

In our model we use the condition of equilibrium to construct the phase diagrams, but the calculated surface pressures are not equal for the coexisting phases. By allowing this deviation from equation (23), we are now able to fit the known phase diagrams. Rationale for this approach is provided by the fact that, in the single component systems, the transition pressure is not always exactly 50 dynes/cm. Other contributions to the surface pressure presumably make up the difference so that equation (23) is satisfied for the net surface pressure. The resulting phase diagrams of binary mixtures are shown in Figure 9 for DMPC - DPPC, Figure 10 for DMPC - DSPC, and Figure 11 for DPPC - DSPC. In these figures, the circles represent the surface pressures which are calculated from equation (22). The temperatures and compositions in our calculations for DMPC - DPPC and DMPC - DSPC correspond to the calorimetric data of Mabrey and Sturtevant (3), and for DPPC - DSPC corresponds to the ESR data of Schimshick and McConnell (22). We shall discuss and explain our results in more detail in a later chapter.

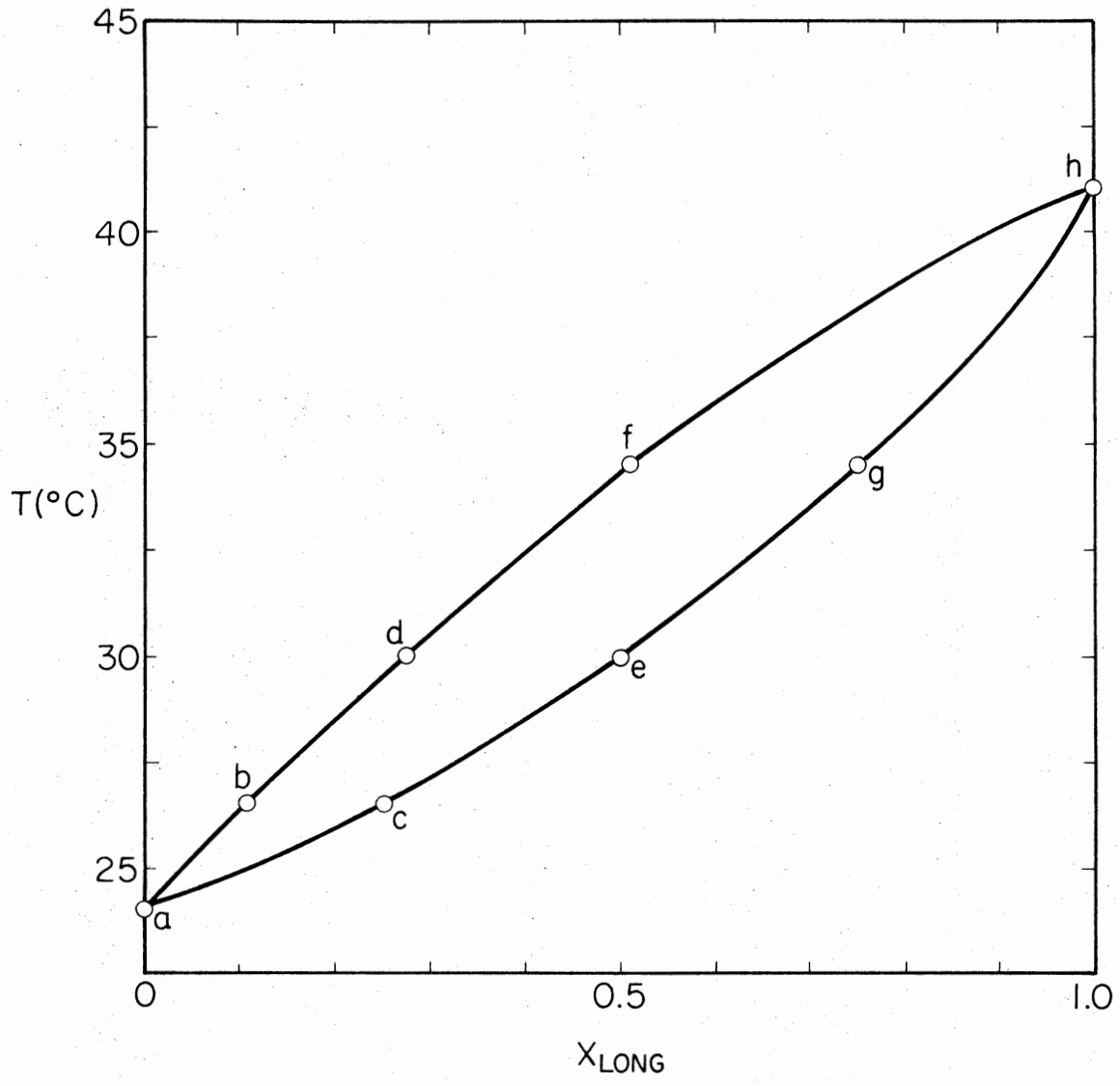

Figure 9. A Theoretical Phase Diagram for DMPC and DPPC Lipid Mixtures. X_{long} is the Mole Fraction of the Long Chain Component. The Solid Lines Correspond to the Calorimetric Data of Mabrey and Sturtevent (3), and the Circles Represent the Surface Pressure Which are Calculated from Equation (22). These Surface Pressure (Dynes/cm) are a = 49, b = 50, c = 48, d = 50.5, e = 47.5, f = 51, g = 47, and h = 50

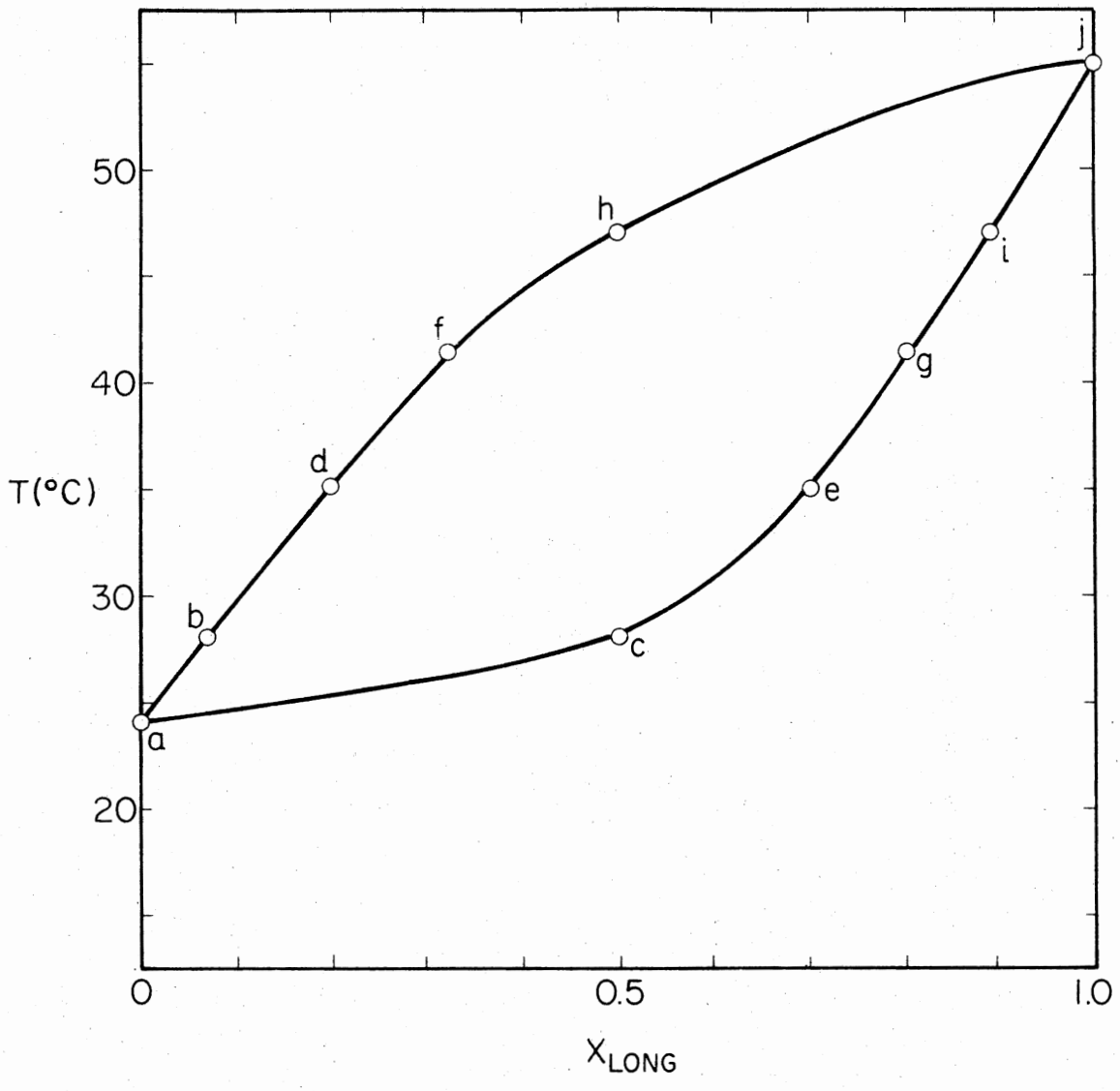

Figure 10. A Theoretical Phase Diagram for DMPC and DSPC Phospholipid Mixtures. X_{long} is the Mole Fraction of the Long Chain Component. The Solid Lines Correspond to the Calorimetric Data of Mabrey and Sturtevent (3), and the Circles Represent the Calculated Surface Pressure. These Surface Pressures (Dynes/cm) are a = 49, b = 51, c = 38, d = 55, e = 40, f = 58, g = 46, h = 59, i = 48, and j = 52

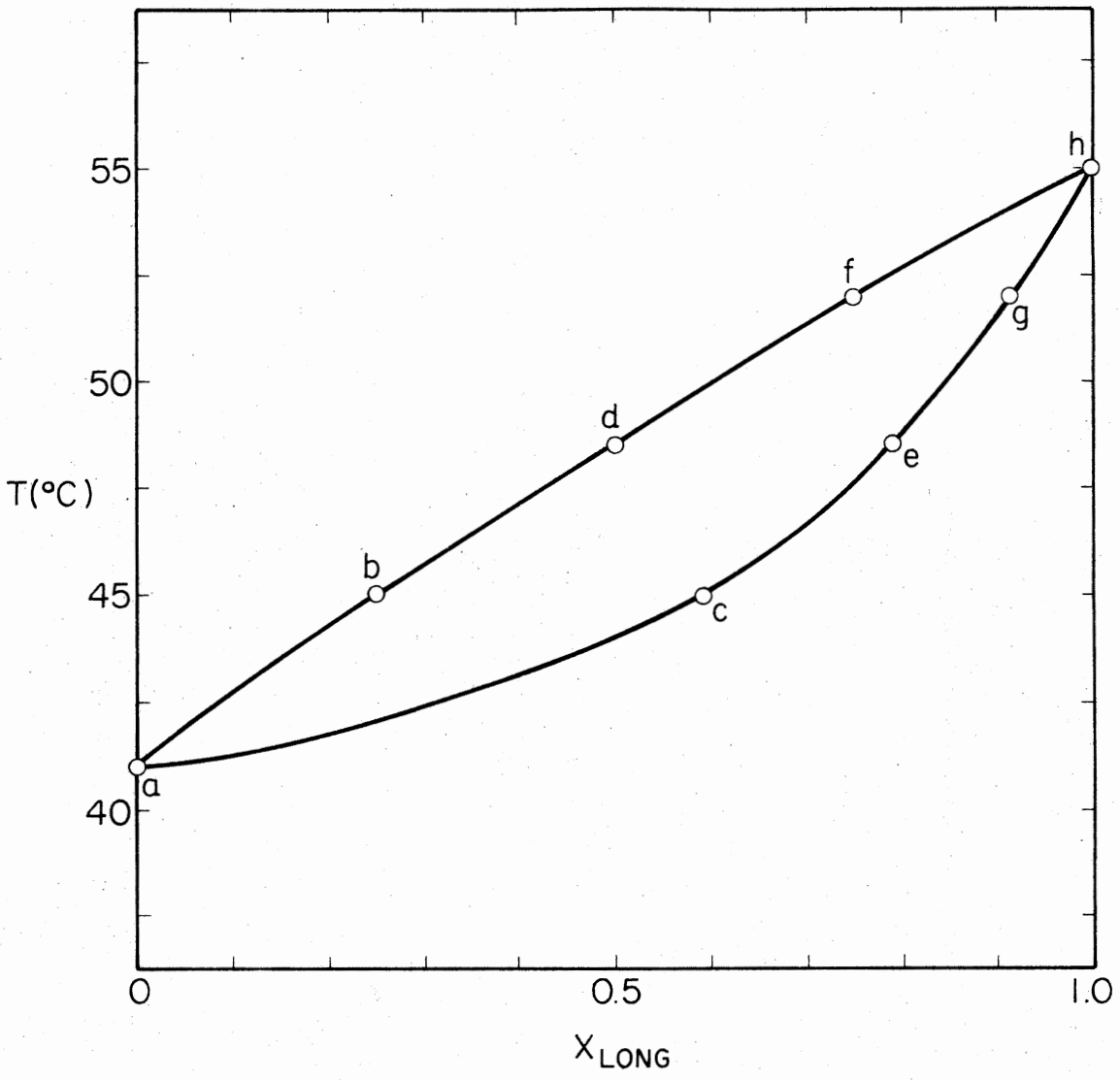

Figure 11. A Theoretical Phase Diagram for DPPC and DSPC Phospholipid Mixtures. X_{long} is the Mole Fraction of the Long Chain Component. The Solid Lines Correspond to the ESR Data of Shimshick and McConnell (23), and the Circles Represent the Calculated Surface Pressure. These Surface Pressures (Dynes/cm) are a = 50, b = 50, c = 47, d = 51.5, e = 48, f = 53, g = 51, and h = 52

Mixtures of Lipid and Cholesterol

Cholesterol is recognized as an important component of biological membranes in animal cells. Many studies have shown that the lipid properties, affected by introduction of cholesterol (12,29-32). It is known that the incorporation of cholesterol into multibilayers decreases the fluidity of hydrocarbon chains above phase transitions. The disappearance of transition seems to be due to the rigid nature of hydrocarbon chains of the lipid. It is also possible that some hydrogen bonding occurs between hydroxyl groups of cholesterol and carbonyl oxygen groups of phospholipids (73). The hydrogen bonded structure may reduce the number of gauche conformations in lipids. Some aspects of this behavior can be simulated by studying the steric portion of the cholesterol interaction.

From the experimental results (12,29-32,73) it is suggested that we might alter the lipid chain phase transition by including cholesterol as another hard cylinder in our mixtures. Then the total free energy of C_{16} - cholesterol mixtures is given by

$$F/NKT = \frac{500}{RT}\left(\sum_{i=1}^{8} g_i \alpha_i\right) - \frac{C(16)}{RT\left[A - (38\, X_{10} + A_o\, X_{ch})\right]^{1.5}} \tag{24}$$

$$- \left\{1 - \sum_{i=1}^{8} \alpha_i \ln(\alpha_i / W_i) + \ln\left(A - \sum_{i=1}^{8} \alpha_i A_i\right) - \frac{\left(\sum_{i=1}^{8} \alpha_i \sqrt{A_i}\right)^2}{\left(A - \sum_{i=1}^{8} \alpha_i A_i\right)}\right\}$$

The summation from one to seven in this equation correspond to a C_{16} bilayer and state number eight corresponds to cholesterol. Because the cholesterol molecule is smaller in cross section than double-chain

lipid molecule, we chose the cholesterol parameters, $g_8 = 0$, $W_8 = 1$, and $A_8 = 35\ \mathring{A}^2$ (74). Here X_{16} is the fixed composition of lipid and X_{ch} is the fixed composition of cholesterol. The A_o is the average close-packed area for cholesterol molecule, to be evaluated semiempirically. Since we consider only the hard-core interaction between lipid and cholesterol molecules, the mean packed area, $38\ X_{16} + A_o\ X_{ch}$ must be used for attractive energy in equation (24). Using the same reasoning in the single-component system, we consider the ratio of the excluded volume interaction to the long range interaction in equation (24)

$$r = \lim_{A \to 35} \left| \frac{1/(A - 35)}{1/[A - (38\ X_{16} + A_o\ X_{ch})]^{1.5}} \right| \tag{25}$$

$$= \lim_{A \to 35} \left| \frac{[A - (38\ X_{16} + A_o\ X_{ch})]^{1.5}}{(A - 35)} \right|$$

That is $38\ X_{16} + A_o\ X_{ch}$ in equation (24) smaller than 35. Using $X_{16} + X_{ch} = 1$, we can write

$$38\ (1 - X_{ch}) + A_o\ X_{ch} < 35 \tag{26}$$

or

$$3 < X_{ch}\ (38 - A_o) \tag{27}$$

According to the studies of Forslind and Kjellander (74), the amount of cholesterol should vary only in the interval $0 \leq X_{ch} < 0.5$. Hence, we have

$$3 < X_{ch}\ (38 - A_o) < \tfrac{1}{2}\ (38 - A_o) \tag{28}$$

This suggests $A_o \lesssim 32$ Å^2. In our studies we use $A_o = 30$ Å^2. This figure is slightly less than 35 Å^2 used for the ground state in the hard-core interactions. Results of the lipid-cholesterol are plotted on Figure 12.

Mixtures of Lipid and Protein

Proteins are the most important constituents of cell membranes. It is clear that proteins mediate most of the important biochemical functions that membranes perform. An understanding of the interactions between lipid and protein is therefore essential to an understanding of how membranes work.

Of the three classes of protein-lipid interactions discussed in the introduction, only the third promises a straightforward incorporation into a theoretical model of type described here. Protein molecules in this class occupy volume in the hydrocarbon chain region so that an increasing immobilization of lipid molecules around protein molecules occurs which can cause the phase transition of the lipid to vanish. Theoretical treatment of lipid-protein interactions is similar to the lipid-cholesterol interactions except that the dimensions of protein molecules are much greater than lipid molecules. Following the same reasoning used in the previous part, we consider the hard-core interactions between lipid and protein molecules, and write the free energy of DPPC - protein mixtures as

$$F/NKT = \frac{500}{RT}\left(\sum_{i=1}^{8} g_i\alpha_i\right) - \frac{C(16)}{RT\left[A - (38\,X_{16} + 105\,X_{po})\right]^{1.5}} - \left\{1 - \sum_{i=1}^{8}\alpha_i \ln(\alpha_i/W_i) + \ln\left(A - \sum_{i=1}^{8}\alpha_i A_i\right) - \frac{\left(\sum_{i=1}^{8}\alpha_i\sqrt{A_i}\right)^2}{\left(A - \sum_{i=1}^{8}\alpha_i A_i\right)}\right\} \tag{29}$$

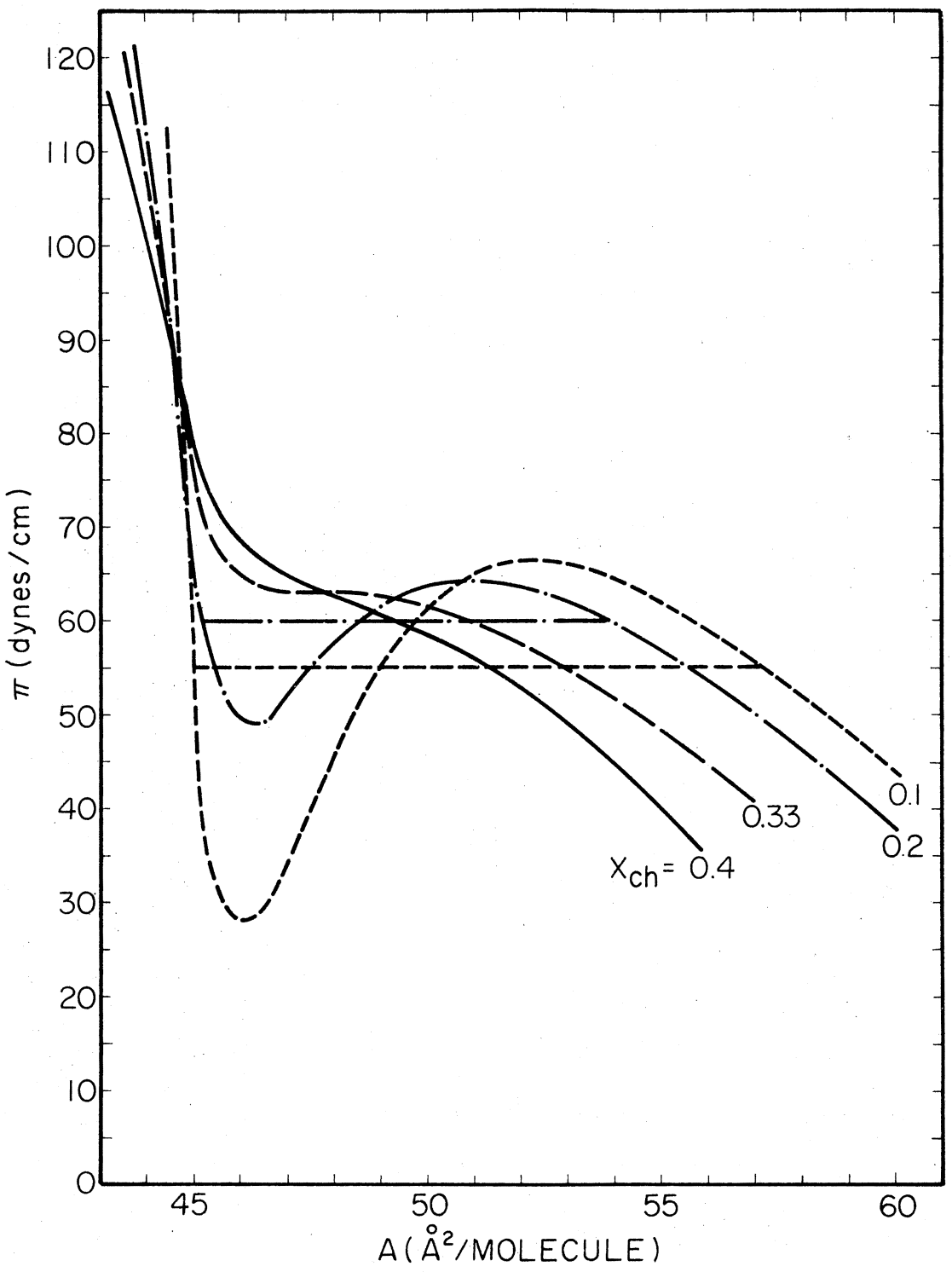

Figure 12. Monolayer Isotherms for DPPC-Cholesterol Mixtures, for Various Cholesterol Mole Fractions at T = 314°K. The Transition Vanishes as the Mole Fraction of Cholesterol Approaches 33%. In This Model, the Cholesterol is Considered to be a Hard Cylinder of Area 35 Å^2

The summation from one to seven in this equation corresponds to a DPPC bilayer and state number eight corresponds to protein state. According to the studies of Chapman et al. (37), the packing of polyptide gramicidin A and hydrocarbon chain is in a hexagonal array. The diameter of gramicidin A corresponds to a size of 11.8 $\mathring{A}$. Therefore, we chose protein parameters, $g_8 = 0$, $A_8 = 110\ \mathring{A}^2$, $W_8 = 1$ in our calculation. The $38\ X_{16} + 105\ X_{pr}$ is the mean packed area of hard-core system. Here the fixed composition of lipid is X_{16}; protein is X_{pr}. Using the semiempirical construction again, we chose the average close-packed area for the protein molecule $A_o = 105\ \mathring{A}^2$/molecule. This figure is slightly less than 110 $\mathring{A}^2$/molecule used for the ground state in the hard-core interactions. Because the dimension of the protein molecule is greater than lipid molecule, we also considered the protein area, $A_8 = 230\ \mathring{A}^2$ and $A_8 = 1000\ \mathring{A}^2$ in our calculations. The average close-packed areas for protein molecules (A_o) were chosen to be 228 $\mathring{A}^2$ and 800 $\mathring{A}^2$ respectively in these computations. Results of the lipid-protein interactions are plotted on Figures 13, 14, and 15.

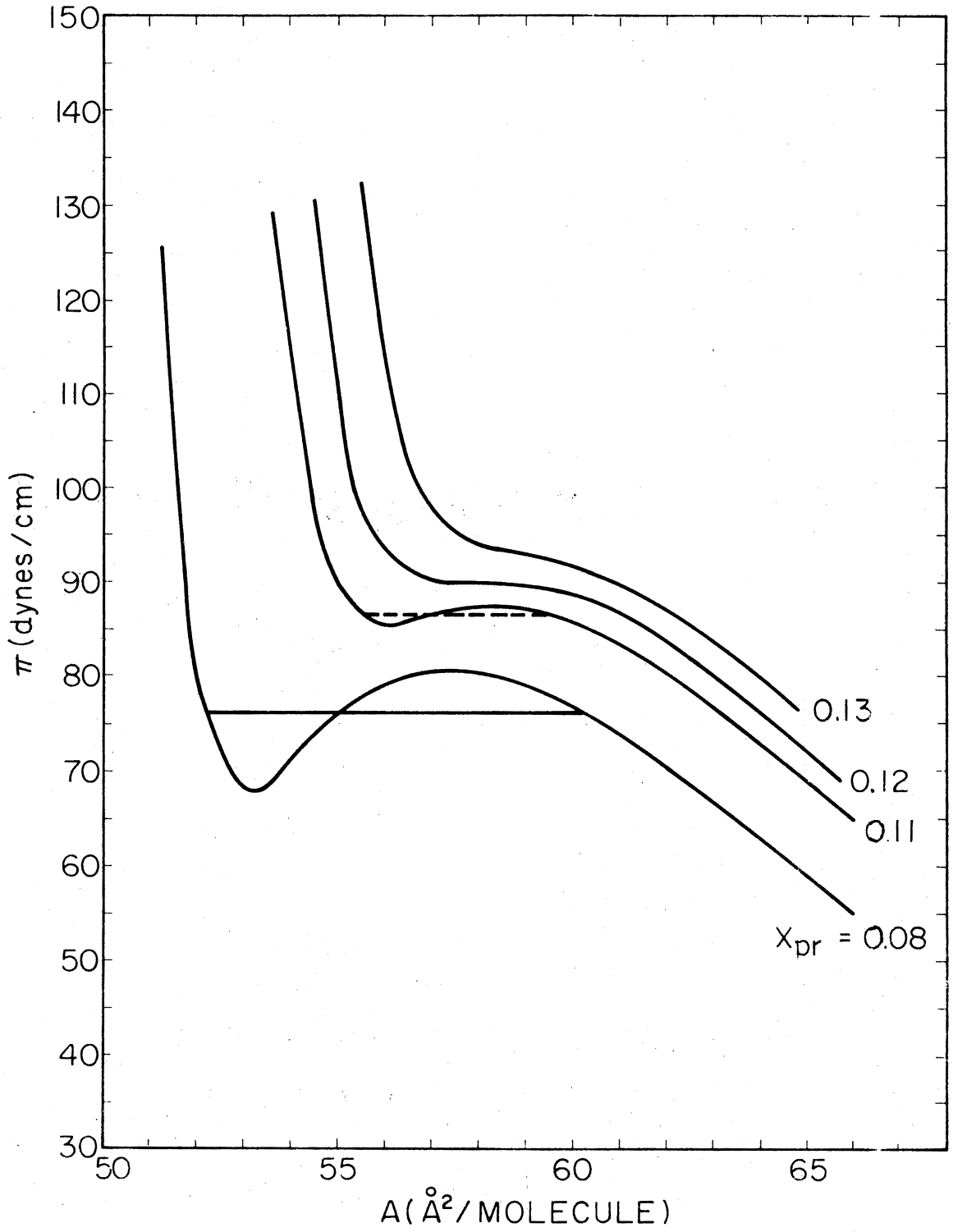

Figure 13. Monolayer Isotherms for DPPC-Protein Mixtures With the Indicate Mole Percents of Protein at T = 314°K. Using a Protein Area 110 Å^2, Corresponding to Gramicidin A, the Transition Disappears at About 12 Mole Percent of Protein

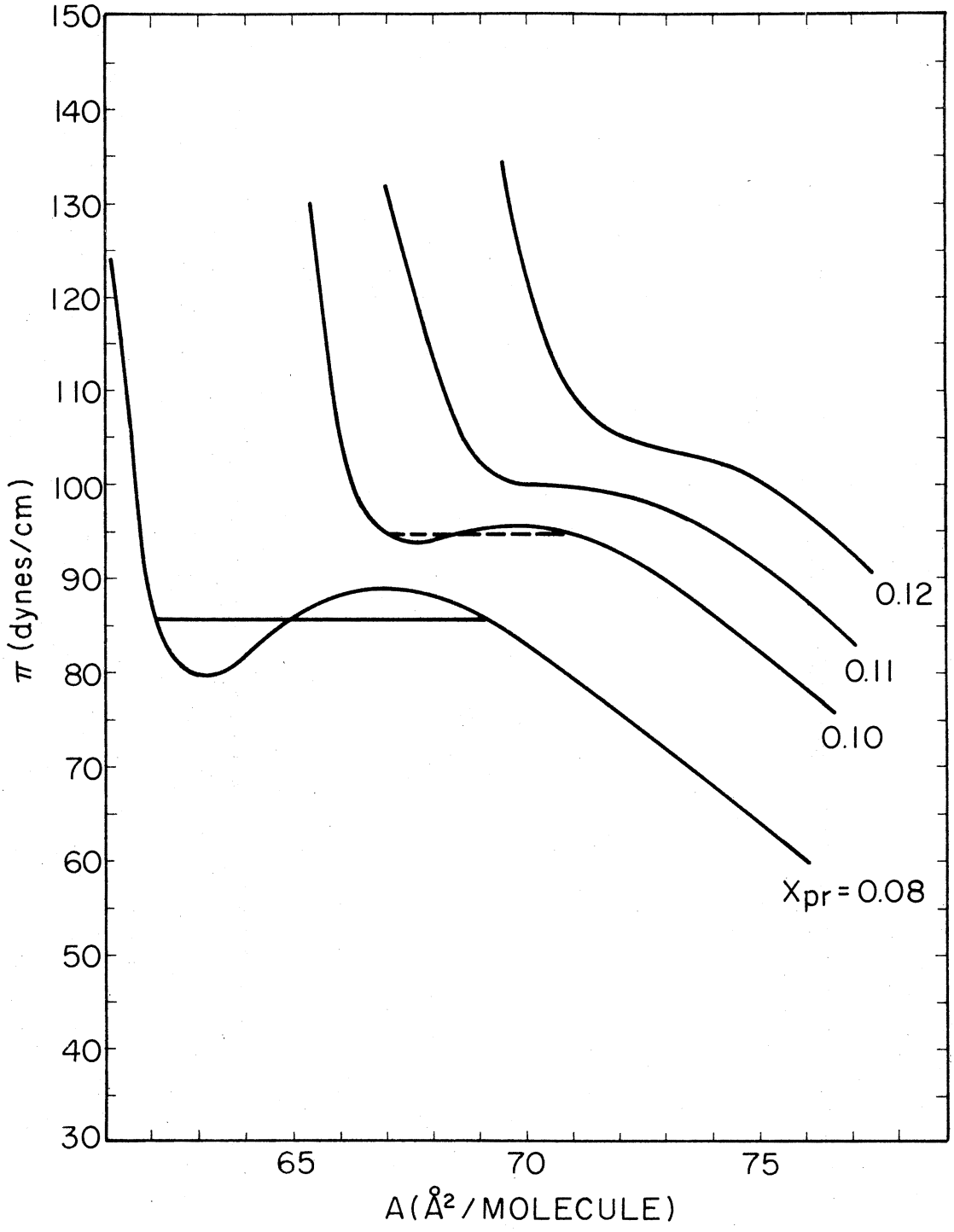

Figure 14. Monolayer Isotherms for DPPC-Protein Mixtures, for Various Protein Mole Percents at T = 314°K. The Protein Area Used Here is 230 Å^2, and the Transition Vanishes at About 11 Mole Percent of Protein

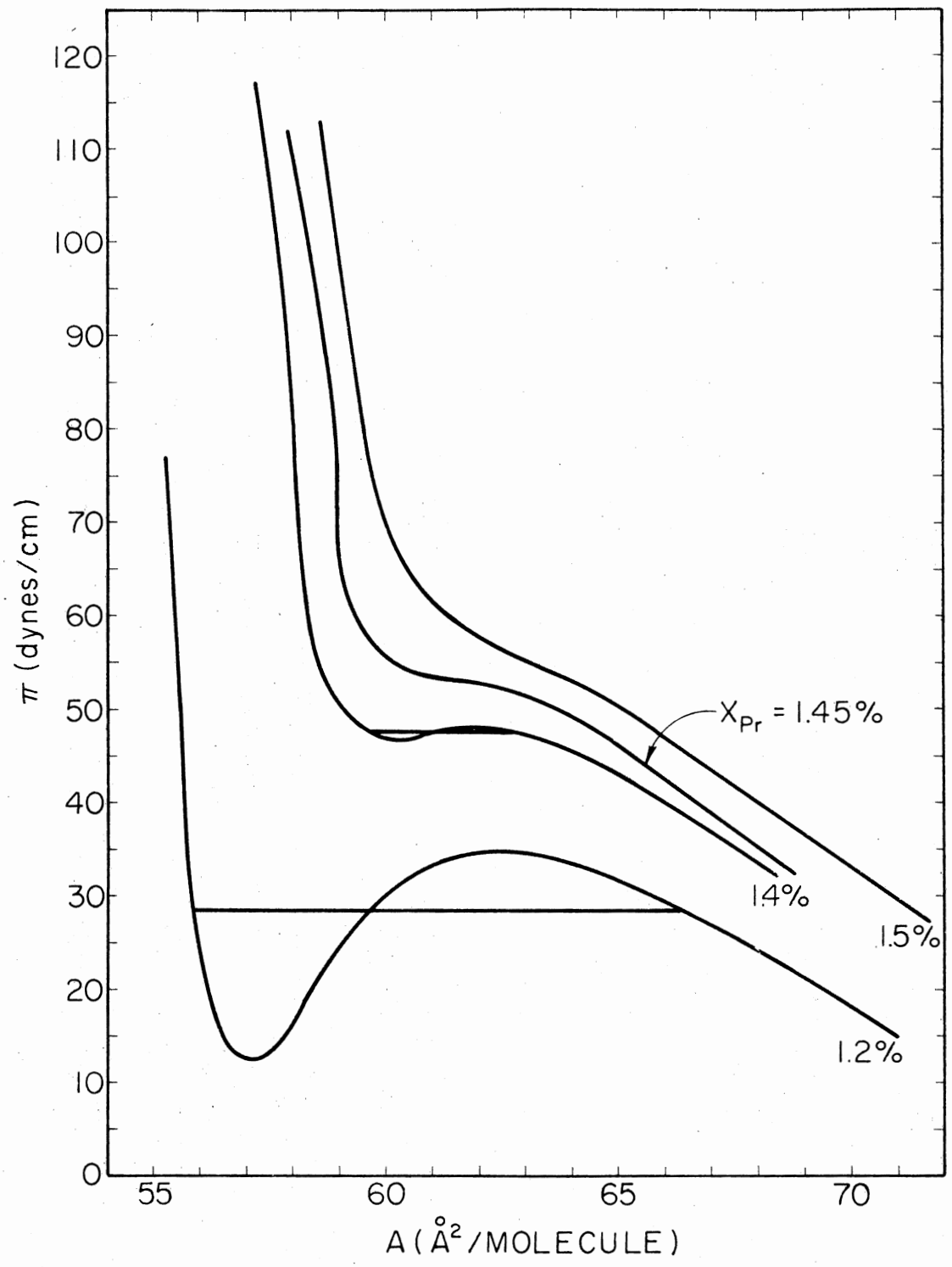

Figure 15. The Pressure-Area Isotherms for DPPC-Protein Mixtures, for Various Mole Percents of Protein at T = 314°K. The Protein Area Used Here is 1000 $Å^2$, and the Transition Disappears at About 1.45 Mole Percents of Protein

CHAPTER IV

RESULTS AND DISCUSSIONS

One-Component Systems

The results of our calculation surface pressures, area and enthalpy changes of DMPC, DPPC, DSPC, and DBPC are listed in Table V. From this table, the model gives enthalpy changes that are in good agreement with experiment (2,3,4). The experimental area changes across the transition for these molecules are on the order 20 ~ 35% (1,65). The calculated area changes in the model are in reasonable agreement with the experiment. The molecular packing of a bilayer corresponds to that of precursor monolayer at a surface pressure of 47 ~ 50 dynes/cm (40,75). The calculations of the surface pressures in the model are in quite good agreement with the cariectureal values (40).

These results indicate that the model has succeeded in describing the one-component lipid phase transitions by using only one freely adjustable parameter, the van der Waals energy constant, with an effective interaction function. The main motivation of this work is, however, to consider mixtures of lipid with lipid, protein, and cholesterol.

Binary Mixtures of Lipid

So far very little attention has been paid to mixed monolayers by the experimentalists though such detailed studies would be of considerable interest. We thus directly compare the calculated thermodynamic

TABLE V

EXPERIMENTAL AND CALCULATED PHASE TRANSITION PROPERTIES OF PHOSPHATIDYLCHOLINE

Lipid	Acyl Chain Length	Transition Temperature (^{o}K)	ΔH(Kcal/mole)		ΔA(%)		π(dynes/cm)	
			Exp.	Calc.	Exp.	Calc.	Esti.	Calc.
DMPC	C_{14}	297[a]	5.4[a]	6.3	20~35[c]	34.5	~ 50[d]	49
DPPC	C_{16}	314[a]	8.7[a]	8.6	20~35[c]	39.8	~ 50[d]	50
DSPC	C_{18}	328[a]	10.6[a]	11.2	20~35[c]	42.8	~ 50[d]	52
DBPC	C_{22}	348[b]	14.9[b]	14.3	20~35[c]	40.3	~ 50[d]	52.5

[a] Reference 3.

[b] Reference 4.

[c] Reference 1, 65.

[d] Reference 40, 75.

properties of mixed monolayers with the experimental data of Phillips et al. (76). The results of area-mole fraction of short chain component for mixed monolayers of DPPC - DSPC, DMPC - DSPC, and DMPC - DPPC lipids are shown in Figures 6, 7 and 8 at pressures 5 and 20 dynes/cm. The plots of area versus mole fraction of short chain component diagrams for mixed DPPC - DSPC monolayers do not completely agree with experiment, since the surface pressure-area isotherm in our model at surface pressure 20 dynes/cm has a discontinuity which is due to the first order phase transition, and since the experimental curves have continuous slopes.

As we described previously, phase diagrams representing lateral phase separation in the plane of a lipid bilayer can be described as two-dimensional equilibria between the fluid and solid phases. The phase diagrams in our model are constructed by the condition of equilibrium such that temperature, surface pressures, and chemical potential at equilibrium have the same values for fluid and solid phases. As mentioned previously, without adjustable surface pressures, no phase diagrams can be found in this model. The phase diagrams of binary lipid mixtures in our model are shown in Figures 9, 10, and 11. In these Figures the solid lines correspond to the experimental data, and the circules represent the surface pressures which are calculated from equation (22). From these figures, the calculations of the hydrocarbon chain pressures are not the same for the coexisting phases but are allowed to vary so that the experimental data may be fit. This is because in pure lipid monolayers the pressure should be, it seems, slightly different for the different numbers of the homologous series. Therefore in a mixture it may be that the chain pressure is slightly different for two points at the same T on a phase diagram. Due to the complicated nature of interac-

tions between the head group and water near the head groups, we expect that a slight adjustment in this surface contribution to the pressure can make up the difference. Then the differences in total surface pressure and chemical potential between coexisting phases at same temperature on a phase diagram will be zero as required.

Hence, a complete quantitative in our model would consider two parts of the surface pressure (43-44); the hydrocarbon chain pressure and hydrophobic forces at the interface with the bulk water.

Mixtures of Lipid-Cholesterol and Lipid-Protein

The calculated pressure-area isotherms for mixtures of DPPC - cholesterol are shown in Figure 12. We find that the addition of cholesterol to lipid causes the phase transition of the phospholipid to disappear at cholesterol composition $X_{ch} = 0.33$. This result is in excellent agreement with experiment (30). Because of the cholesterol effect, sharp phase transitions would be expected to occur only in bilayers that are not rich in cholesterol.

The calculated pressure-area isotherms for mixtures of DPPC - protein are shown in Figures 13, 14, and 15. These figures show the addition of protein to lipid causes the phase transitions of lipid to vanish at about protein composition, 0.014, 0.11, and 0.12, where the protein areas are taken to be 1000, 230, and 110 $\mathring{A}^2$ respectively and the values of A_o are accordingly adjusted. These results can be compared with experimental results for the third class of protein (33). By comparing the results of Figure 13 with the experimental data of Chapman et al. (37), we find that our calculation is in good agreement with the experiment.

CHAPTER V

CONCLUSIONS

Using the scaled particle theory, the semiempirical attractive potential, and the rotational isomeric theory, we have presented a reliable model to describe lipid bilayer phase transitions. The model Hamiltonian which simplifies the exact intermolecular interactions by using the semiempirical potentials is obtained from the results of experimental studies of lipid bilayer phase transitions and the theoretical consideration of attractive energy. The most important and difficult part in the calculation of lipid-bilayer phase transitions is the hard-core interactions between molecules. The model in our calculations works very well. This is because the scaled particle theory (SPT) gives a good approximation for describing the hard-core systems. Recently SPT has been usefully employed in the theory of liquid crystal phase transitions (77-79).

An advantage of our model in the hard-core interactions is that, unlike applications to sphero-cylindrical molecular systems (77-79), a direct application of the scaled particle approach results in a thermodynamic consistency in the Maxwell relation which has been shown in Appendix A. A disadvantage of the model arises in that a straightforward application of the scaled particle expression requires a singular long range attractive force in order to obtain phase transition. Although the hard-core area in the singular potential is an important

parameter in our model to determine the bilayer phase transition, the manner by which we soften the hard core is of necessity somewhat arbitrary. We make this choice in a manner which is quite consistent with the physical properties of the system, however, as described earlier.

Although our model has successfully described lipid bilayer phase transitions there are two deficiencies in the model. First, the effective potentials cannot easily be compared with realistic intermolecular potentials. This is because the solutions we presented here are approximate. Secondly, the usual way to describe the coexisting phase of binary lipid mixtures by generating T-X curves from double tangents in the G-X curves is not possible in this model. The Gibbs free energy at fixed T, N, and π does not allow a double-tangent construction. Thus in the simple model, which is basically a mixture of many types of hard disks, biphasic behavior is not possible at fixed pressure π. The reason for the failure of the double-tangent construction is that of the surface pressure is not actually controlled in an experiment, so it cannot be fixed in our calculation. One does not expect strong variation of π with X and T but same change does seem likely. In an experiment, A and π at equilibrium will adopt the values which minimize the Gibbs free energy. In the model we present here we have not considered the other possible contributions to the energy of lipid bilayers such as the head group and water interactions. Hence, we do not expect to reproduce completely the experimental results in our calculation. However, because of the complex nature of interactions between the head group and water, we can only use a phenomenological pressure to make up for the deficiency in our model. Thus the head group-water contributions to the surface pressure refers to an adjustable parameter, and then the result of total

surface pressures (hydrocarbon chain and hydrophobic pressures), would fix the known phase diagrams. As we described in the introduction, the hypothesis of thermodynamic independence of the hydrocarbon chain and head group regions in a monolayer has been tentatively supported by Monte Carlo computer experiments (52). Our conclusion in our model for two-component systems is that one cannot apply the double-tangent method to obtain the phase diagrams, but with the additional phenomenological assumption concerning surface pressures the model can describe the phase diagrams of binary mixtures of lipids. The model also does not seem to work very well in mixed monolayers. In one-component systems, the model has succeeded in describing the lipid-bilayer phase transitions by using only one (van der Waals energy constant) freely adjustable parameter. In two-component systems, we have still used this parameter to describe the binary mixtures of lipids. Since the attractive ratio of energy constants to the temperature in the one-component model are adjustable at the chain melting transition, the attractive energy in our two-component model is too large to study the mixed monolayers at lower temperature, $295^{o}K$, than the chain transition temperature.

To test further results of our calculations, we have extended the model to the description of lipid-cholesterol and lipid-protein mixtures. As we described in Chapter III, the rigid nature of cholesterol prevents the cooperative isomerization of the hydrocarbon chains of the lipids, and the hydrophobic protein of gramicidin A occupying a volume in the hydrocarbon chains region increases the immobilization of lipid molecules around protein molecules. From these facts we suggest that consideration of only the hard-core interactions between lipid-cholesterol and lipid-protein molecules in our model give us a good approximation to

the experimental results of the effect of cholesterol and protein on the lipid phase transition. Our main conclusion from our calculation is that the model works well in describing the mixture of lipid-cholesterol and lipid-protein mixtures with a freely adjustable parameter concerning the hard-core area.

Because of the singular nature of the long range attractive force in our model, it is difficult to compare the model with a realistic intermolecular potential. It seems that an improvement of our theoretical model should carefully consider the explicit long range forces of the interactions among the lipid molecules. Using the original scaled particle theory, an expression for the total partition function could be derived which treats the individual interaction separately. From the partition function, the packing entropy, the long range forces, and the internal energy of lipid molecules can be found. Then the result of the free energy would be closer to the realistic intermolecular potential, and the thermodynamic properties of lipid bilayers would be obtained as we presented in Chapter IV.

In conclusion, the model we presented here has, with some success, interpreted the experimental data of lipid systems and has increased our understanding of the structural properties of the biological membranes of lipid bilayers, lipid mixtures, lipid-cholesterol, and the lipid-protein interactions.

REFERENCES

1. Engelment, D. M., J. Mol. Biol. 47, 115 (1970) and 58, 153 (1971).

2. Hinz, H. J. and Sturtevant, J. M., J. Biol. Chem. 247, 6071 (1972).

3. Mabrey, S. and Strutevant, J. M., Proc. Nat. Acad. Sci. (USA) 73, 3862 (1976).

4. Phillips, M. C., Williams, R. M. and Chapman, D., Chem. Phys. Lipids 3, 234 (1969).

5. Nagle, J. F. and Wilkinson, D. A., Biophys. J. (to be published).

6. Overath, P. and Träuble, H., Biochemistry, 12, 2625 (1973).

7. Penkett, S. A., Flook, A. G. and Chapman, D., Chem. Phys. Lipids, 2, 273 (1968).

8. Seelig, J. and Gally, H. U., Biochemistry, 15, 5199 (1976).

9. Hubbell, W. L. and McConnell, H. M., J. Am. Chem. Soc. 93, 314 (1971).

10. Sackmann, E. and Träuble, H., J. Am. Chem. Soc., 94, 4482 (1972); 94, 4492 (1972) and 94, 4499 (1972).

11. Asher, I. M. and Levin, I. W., Biochim. Biophys. Acta, 468, 63 (1977).

12. Gaber, B. P. and Peticolas, W. L., Biochim. Biophys. Acta. 465, 260 (1977).

13. Faucon, J. F. and Lussan, C., Biochim. Biophys. Acta., 307, 459 (1973).

14. Wilson, G. and Fox, C. F., J. Mol. Biol., 55, 49 (1971).

15. Linden, C. D., Wright, K. L., McConnell, H. M. and Fox, C. F., Proc. Nat. Acad. Sci. (USA), 70, 2271 (1973).

16. Thilo, L., Overath, P., Biochemistry, 15, 328 (1976).

17. Esfahani, M., Limbrick, A. R., Knutton, S., Oka, T. and Wakil, S. J., Proc. Nat. Acad. Sci. (USA), 68, 3180 (1971).

18. Mavis, R. D. and Vagelos, P. R., J. Biol. Chem., 247, 652 (1972).

19. Morrisett, J. D., Pownell, H. J., Plumlee, R. T., Smith, L. C., Zehner, Z. E., Esfahani, M. and Wakil, S. J., J. Biol. Chem. 250, 6969 (1975).

20. Ladbrooke, B. D. and Chapman, D., Chem. Phys. Lipids 3, 304 (1969).

21. Rothman, J. E., J. Theoret., Biol., 37, 1 (1973).

22. Flory, P. J., Statistical Mechanics of Chain Molecules, New York, Wiley, Interscience (1969).

23. Shimshick, E. J. and McConnell, H. M., Biochemistry, 12, 2351 (1973).

24. Chapman, D., Urbina, J. and Keough, K. M., J. Biol. Chem., 249, 2512 (1974).

25. Petit, V. A. and Edidin, M., Science, 184, 1183 (1974).

26. Kleemann, W. and McConnell, Biochim. Biophys. Acta, 345, 220 (1974).

27. Wu, S. H. W. and McConnell, H. M., Biochemistry, 14, 847 (1975).

28. Lee, A. G., Biochim. Biophys. Acta, 413, 11 (1975).

29. Ladbrooke, B. D., Williams, R. M. and Chapman, D., Biochim. Biophys. Acta, 150, 333 (1968).

30. Hinz, H. J. and Sturtevant, J. Mol. Biol., 247, 3697 (1972).

31. Shimshick, E. J. and McConnell, H. M., Biochem. Biophys. Res. Commun., 53, 446 (1973).

32. Kleemann, W. and McConnell, H. M., Biochim. Biophys. Acta, 419, 206 (1976).

33. Papahadjopoulos, D., Moscarello, M., Eylar, E. H. and Isac, T. Biochim. Biophys. Acta, 401, 317 (1975).

34. Gennis, R. B. and Jonas, A., Ann. Rev. Biophys. Bioeng., 6, 195 (1977).

35. Longmuir, K. J., Capaldi, R. A. and Dahlquist, F. W., Biochemistry, 16, 5746 (1977).

36. Dahlquist, F. W., Muchmore, D. C., Davis, J. H. and Bloom, M., Proc. Nat. Acad. Sci. (USA), 74, 5435 (1977).

37. Chapman, D., Cornell, B. A., Eliasz, A. W. and Perry, A., J. Mol., Biol., 113, 517 (1977).

38. Nagle, J. F., J. Chem. Phys., 58, 252 (1972).

39. Nagle, J. F., J. Chem. Phys., 63, 1255 (1975).

40. Nagle, J. F., J. Membr. Biol., 27, 233 (1976).

41. Marčelja, S., Biochim. Biophys. Acta, 367, 165 (1974).

42. Scott, H. L., J. Chem. Phys., 62, 1347 (1975).

43. Scott, H. L., Biochim. Biophys. Acta, 406, 329 (1975).

44. Scott, H. L. and Cheng, W. H., J. Col. Int. Sci., 62, 125 (1977).

45. Jacobs, R. E., Hudson, B. S. and Andersen, H. C., Proc. Nat. Acad. Sci. (USA), 72, 3993 (1975).

46. Jacobs, R. E., Hudson, B. S. and Andersen, H. C., Biochemistry, 16, 4349 (1977).

47. McCammon, J. A. and Detuch, J. M., J. Am. Chem. Soc., 97, 6675 (1975).

48. Marsh, D., J. Membr. Biol., 18, 145 (1974).

49. Jackson, M. B., Biochemistry, 15, 2555 (1976).

50. Marčelja, A., J. Chem. Phys., 60, 3599 (1974).

51. Phillips, M. C. and Chapman, D., Biochim. Biophys. Acta, 163, 301 (1968).

52. Scott, H. L. and Cherng, S. L., Biochim. Biophys. Acta, (to be published).

53. Träuble, H. J. Membr. Biol. 4, 193 (1971).

54. Salem, L., J. Chem. Phys., 37, 2100 (1962).

55. Devaux, P. and McConnell, H. M., Am. Chem. Soc., 94, 4475 (1972).

56. Scandlla, C. J., Devaux, P. and McConnell, H. M., Proc. Nat. Acad. Sci. (USA), 69, 2056 (1972).

57. Liebman, P. A. and Entine, G., Science, 185, 457 (1974).

58. Seelig, J. and Niederberger, W., Biochemistry, 13, 1585 (1974).

59. Seelig, A. and Seelig, J., Biochemistry, 13, 4839 (1975).

60. Lebowitz, J. L., Helfand, E. and Praestgaard, E., J. Chem. Phys., 43, 774 (1965).

61. Träuble, H., Biomembranes 3, 197 (1973).

62. Pechhold, W., Kolloid Z. Z., Polym., 228, 1 (1968).

63. Hubbell, W. L. and McConnell, H. M., J. Am. Chem. Soc., 93, 314 (1971).

64. McFarland, B. G. and McConnell, H. M., Proc. Nat. Acad. Sci. (USA), 68, 1274 (1971).

65. Träuble, H. and Haynes, D., Chem. Phys. Lipids, 1, 324 (1971).

66. Sheetz, M. P. and Cham, S. I., Biochemistry, 11, 4574 (1972).

67. Tardieu, A., Luzzate, V. and Reman, F. C., J. Mol. Biol., 75, 711 (1973).

68. Schindler, H. and Seelig, J., Biochemistry, 14, 2283 (1975).

69. Longuet-Higgins, H. C., Advan. Chem. Phys., 12, (1967).

70. Buckingham, A. D., Discussions, Faraday, Soc., 40, 232 (1956).

71. Margenan, H. and Kestner, N. R., Theory of Intermolecular Force, Pergamon Press (1971).

72. Gordon, P., Principles of Phase Diagrams in Materials Systems, McGraw-Hill (1968).

73. Huang, C. H., Lipids, 12, 348 (1977) and Nature, 259, 242 (1976).

74. Forslind, E. and Kjellander, R., J. Theor. Biol., 51, 97 (1975).

75. Hui, S. W., Cowden, D., Papahadjopoulos, D. and Parsons, D. F., Biochim. Biophys. Acta, 382, 265 (1975).

76. Phillips, M. C., Ladbrooke, B. D. and Chapman, D., Biochim. Biophys. Acta, 196, 35 (1970).

77. Cotter, M. A., Phys. Rev., A 10, 625 (1974).

78. Cotter, M. A , and Martire, D. E., J. Chem. Phys., 52, 1902 (1970); 53, 4500 (1970).

79. Cotter, M. A., J. Chem. Phys., 66, 1098 (1977).

80. Helfand, E., Frish, H. L. and Lebowitz, J. L., J. Chem. Phys., 34, 1037 (1961).

81. Lebowitz, J. L. and Rowlinsion, J. S., J. Chem. Phys., 41, 133 (1964).

82. Wood, W. W., Physics of Simple Liquids, Edited by Tempreley, H. N. V. et al. (1968), Interscience, New York.

APPENDIX

THE PACKING ENTROPY

The SPT was one of the successful attempts at deriving approximate expression for the chemical potential and pressure of hard-particle fluids. The basic idea of SPT is to consider the reversible work necessary to insert a scaled particle at some arbitrary point in the hard-core fluid. It is exact in one-dimension (60,80) and gives equations of state for two-dimension (60) and three-dimension hard spheres (60,81) that are in good agreement with the Monte Carlo and molecular dynamic experiments (82).

From Scaled Particle Theory (60) the equation of state and chemical potential are given by

$$\beta P = \left[\frac{\Sigma\rho_i}{(1 - \pi \sum_i \rho_i R_i^2)}\right] + \left[\frac{\pi(\Sigma\rho_i R_i)^2}{1 - \pi \sum_i \rho_i R_i)^2}\right] \qquad \text{(a)}$$

$$\beta\mu_i = K T \ln\left[\rho_i \frac{h^3}{(2\pi m_i kT)^{3/2}}\right] + \{- \ln[1 - \pi \sum_i \rho_i R_i^2] \qquad \text{(b)}$$

$$+ \left[\frac{2\pi(\sum_i \rho_i R_i) R_i}{(1 - \pi \Sigma \rho_i R_i^2)}\right] + \beta \pi \rho R_i^2$$

Where P is the pressure, μ_i is the chemical potential of ith species, ρ_i and R_i are the density and radius of a particle of the ith species respectively, and β is the reciprocal temperature.

From equations (a) and (b) we can obtain Helmholtz free energy of a mixture of hard disks as a function of T, A, A_i, and α_i.

The Helmholtz free energy, F, is

$$F = \sum_i N_i/\mu_i - PA$$

$$= \frac{A}{\beta}\left(\beta \sum_i \rho_i \mu_i - \beta P\right) \qquad (c)$$

$$F = \frac{A}{\beta}\left\{\sum_i \rho_i \ln\left[\rho_i \frac{h^3}{(2\pi m_i kT)^{3/2}}\right] - \sum_i \rho_i \left[1 - \pi \sum_i \rho_i R_i^2\right]\right.$$

$$\left. + \frac{2\pi\left(\sum_i \rho_i R_i\right)\left(\sum_i \rho_i R_i\right)}{\left(1 - \pi \sum \rho_i R_i^2\right)} + \beta \pi P \sum_i \rho_i R_i^2 - \beta P\right\}$$

$$= - NKT \left\{1 - \sum_i \alpha_i \ln \alpha_i + \ln\left[\frac{h^3}{(2\pi m_i kT)^{3/2}}\right]\right.$$

$$\left. + \ln\left[A/N - \sum_i \alpha_i A_i\right] - \frac{\left(\sum_j \alpha_j \sqrt{A_j}\right)^2}{\left(A/N - \sum_i \alpha_i A_i\right)}\right\} \qquad (d)$$

Where $A_i = \pi R_i^2$, $\alpha_i = \frac{N_i}{N}$, and $\rho_i = \frac{N_i}{A}$

Here N is the total number of molecules, A is the total area of system, and N_i is the number of particles of species i.

For hard-disk system, the kinetic energy term, $\frac{h^3}{(2\pi m_i kT)^{3/2}}$, can be neglected. Then the Helmholtz free energy is given by

$$F = - NKT \left(1 - \sum_i \alpha_i \ln \alpha_i + \ln\left[A/N - \sum_\lambda \alpha_i A_i\right] - \frac{\left(\sum_j \alpha_j \sqrt{A_j}\right)^2}{\left(A/N - \sum_i \alpha_i A_i\right)}\right) \qquad (e)$$

The equation of entropy change is simply given by

$$S = -\left(\frac{\partial F}{\partial T}\right) A$$

$$= NK\left(1 - \sum_i \alpha_i \ln \alpha_i + \ln\left[A/N - \sum_i \alpha_i A_i\right] - \frac{\left(\sum_j \alpha_j \sqrt{A_j}\right)^2}{\left(A/N - \sum_i \alpha_i A_i\right)}\right) \qquad (f)$$

Recently, the SPT approach has been criticized by Cotter (77). The criticism is that the resulting expressions for the chemical potential were not thermodynamically consistent in the Maxwell relation

$$\left(\frac{\partial \mu_i}{\partial \rho_j}\right)_{T,\rho_{k\neq j}} = \left(\frac{\partial \mu_j}{\partial \rho_i}\right)_{T,\rho_{k\neq i}}$$

where μ_k is the chemical potential and ρ_k is the number density of component K for a multicomponent system. Cotter has obtained the thermodynamic consistency in the Maxwell relation by rederiving the chemical potential of hard-core systems (77-77). After calculation of the Maxwell relation, the model from the equation (b) gave the thermodynamic consistency. The advantage of our model is that it shows that a straightforward application of the scaled particle approach does not lead a thermodynamic inconsistency in the Maxwell relation.

VITA[2]

WOOD HI CHENG

Candidate for the Degree of

Doctor of Philosophy

Thesis: A THEORETICAL MODEL FOR LIPID BILAYER PHASE TRANSITIONS AND PHASE DIAGRAMS

Major Field: Physics

Biographical:

Personal Data: Born in Changhua, Taiwan, Republic of China, June 3, 1944, the son of Mr. and Mrs. P. T. Cheng.

Education: Graduated from Yuangling High School, Changhua, Taiwan, in June, 1963; received Bachelor of Science degree in Physics from Tamkang College of Arts and Sciences, Tamsui, Taiwan, in June, 1968; received Master of Science degree in Physics from National Tsinghua University, Hsinchu, Taiwan, in June, 1970; completed requirements for Doctor of Philosophy degree at Oklahoma State University, Stillwater, Oklahoma, in May, 1978.

Professional Experience: Instructor in the Physics Department of Tamkang College of Arts and Sciences, Taiwan, 1971-1974; Graduate Research Assistant in the Physics Department of Oklahoma State University, Stillwater, Oklahoma, 1974-1978.